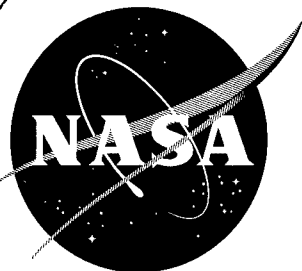B052759

52759

TECHNICAL NOTE

D-1259

UNIFIED NOTCH-STRENGTH ANALYSIS

FOR WROUGHT ALUMINUM ALLOYS

By Paul Kuhn and I. E. Figge

Langley Research Center
Langley Station, Hampton, Va.

NATIONAL AERONAUTICS AND SPACE ADMINISTRATION

WASHINGTON   May 1962

20011221 174

1B

TABLE OF CONTENTS

NATIONAL AERONAUTICS AND SPACE ADMINISTRATION

TECHNICAL NOTE D-1259

UNIFIED NOTCH-STRENGTH ANALYSIS

FOR WROUGHT ALUMINUM ALLOYS

By Paul Kuhn and I. E. Figge

SUMMARY

A simple engineering method is presented for predicting the strength
of notched parts made from wrought aluminum alloys under static loading
or under repeated loading near the fatigue limit. Assumed to be known
are tensile strength, elongation, and modulus of elasticity; in certain
cases, the stress-strain curve must be known; also needed are "Neuber
constants," which are given in the report. Notch configurations ranging
from mild notches to cracks are considered. A large number of compari-
sons between experimental and predicted results are presented.

INTRODUCTION

Almost all component parts of structures and machines incorporate
changes of cross section or notches which act as stress raisers. Elas-
ticians have devoted much attention to the problem of stress concentra-
tion and have provided many solutions based on the theory of elasticity.
Over 20 years ago, sufficient work had been accomplished to justify the
publication of a book by H. Neuber devoted exclusively to the theory of
stresses around notches (ref. 1).

At the same time, a large body of experimental knowledge had been
accumulated by engineers on the strength of notched parts subjected
either to static loading or to fatigue loading. As a result, it was
known long before the publication of Neuber's book that experimental
factors derived from strength tests were always lower than the theoreti-
cal factors derived from the theory of elasticity.

In the static-strength design of metal parts, the elastic theory
of notches was disregarded completely with good justification. Struc-
tural metals cease to be elastic and become plastic before failure takes
place. If the material is assumed to be perfectly plastic, there is no
stress concentration in a notched member; the stress is uniformly dis-
tributed over the net section, and failure may be assumed to take place
when this stress becomes equal to the tensile strength of the material.

This failure "theory" is much simpler than the theory based on the assumption of elasticity - so simple, in fact, that it was used as standard procedure long before there was a formal theory of plasticity - and it has been proven to be adequate for many practical design purposes by a century of experience.

In fatigue-strength design, on the other hand, stress concentrations are very important and must be taken into account - a fact which was established by Wöhler about a century ago from the same set of tests which established definitely that fatigue failure is a problem separate and distinct from static failure. Stress-concentration factors derived from fatigue tests were found to be less than the theoretical ("elastic") factors; this was true even in cases where the peak stress was well within the elastic limit of the material, so that plastic behavior could not be used as the basis of explanation. About 30 years ago, it was established that series of geometrically similar specimens from the same material showed fatigue factors which increased as the size of the specimen increased, and that the fatigue factors appeared to approach the theoretical factor as an asymptotic limit. This "size effect" was ascribed by a number of writers to the fact that engineering metals have a granular structure, whereas the theory of elasticity assumes the material to be a homogeneous continuum, that is to say, devoid of any structure. It will be termed herein the "material size effect" in order to distinguish it from other size effects (which will be discussed briefly later). This term is considered to be more descriptive than the term "geometric size effect" used previously (ref. 2).

Recognizing that theoretical factors are not directly applicable to engineering strength design, Neuber included in his book (ref. 1) a scheme for correcting the theoretical factors to "technical factors" on the basis of a simple theory of material size effect. The correction scheme involves a new materials constant ρ' (termed "Neuber constant" in ref. 3) which must be determined by tests. Neuber evaluated this constant for mild steel from some published high-precision strain measurements on notched specimens; he made no attempt to demonstrate that the "size-corrected factors" are applicable to strength design, either static or fatigue.

Neuber's scheme was developed in reference 3 into a method for predicting fatigue factors applicable to the design of steel parts at stresses near the fatigue limit. A first attempt at a similar application to aluminum alloys (ref. 2) was only moderately successful, partly because the available test data covered a much smaller range of configurations and material properties than the data for steel.

When aircraft accidents focused attention on the problem of estimating the static strength of parts containing fatigue cracks, it was recognized that this problem, also, could be treated by the theory of

size effect together with a suitable theory of placticity effects. A method was published for aluminum alloys (ref. 4) which employed Neuber's scheme for size-effect correction. In addition, however, this method introduced the concept of an "effective tip radius" for cracks, a concept which does not appear in the original Neuber scheme. The Neuber constants appropriate to this method differ somewhat from those that appeared in reference 2 for fatigue applications; it may be well to emphasize that the Neuber constant is not a directly measurable physical quantity, but a mathematical abstraction to which numbers can be assigned only in connection with a well-defined procedure of calculation.

The present paper presents a unified method, employing a single set of Neuber constants applicable to wrought aluminum alloys, for predicting:

(1) The strength of notched parts under repeated loading at zero mean stress near the fatigue limit

(2) The strength of notched parts made from sheet or bar (essentially two-dimensional) under static tensile loading, with main emphasis on sharp notches and cracks

For a method of such wide scope, it is not feasible to arrive at simple and precise numbers for the accuracy of prediction achieved; a large number of test results are therefore shown so that the reader may form his own opinion of the accuracy that may be expected. A simple engineering method for predicting notch strength - fatigue or static - cannot be expected to have a very high accuracy. However, the experimental evidence indicates that errors of prediction attributable to weakness of the method are of the same order as inconsistencies in test results attributable either to imperfect test techniques or to variability of material.

SYMBOLS

a	half-length of internal notch, in.
B	flow-restraint factor (fig. 5)
c	distance from axis of symmetry to base of notch, in.
d	notch depth, in.
E	modulus of elasticity, ksi
$E_{s,n}$	secant modulus corresponding to the net-section stress, ksi

4

$E_{s,p}$ secant modulus corresponding to the peak stress, ksi

$E_{s,u}$ secant modulus corresponding to the stress at the ultimate load, ksi

e elongation in 2-inch gage length, in./in.

K_C theoretical stress-concentration factor for a circular hole in a sheet

K_D theoretical stress-concentration factor for a deep notch

K_F stress-concentration factor effective in fatigue

K_N stress-concentration factor corrected for size effect (Neuber factor)

K_P stress-concentration factor in plastic range

K_S theoretical stress-concentration factor for a shallow notch

K_T theoretical stress-concentration factor

K_{TN} asymptotic limit of K_N as $\rho \to 0$

K_u static notch strength factor

K_u^* calculated static notch strength factor corrected for flow restraint

k elongation correction factor

N number of cycles

S_u tensile strength of notched specimen in which buckling is prevented (based on net section before loading starts), ksi

S_u^* tensile strength of notched specimen in which buckling is not prevented, ksi

t specimen thickness, in.

w specimen width, in.

ρ notch radius, in.

L 1 7 4 3

ρ' material constant (Neuber constant), in.

σ_u ultimate tensile strength, ksi

σ_y yield strength (0.2-percent offset), ksi

ω flank angle, radians or deg

ω_e effective flank angle, radians or deg

METHOD OF CALCULATION

Outline of Method

The distribution of stress over the net section of a notched part is not uniform. Following conventional practice, a nominal stress on the net section is calculated by elementary theory. The peak stress in the section (at or near the root of the notch) can then be expressed as the product of the nominal net-section stress and a factor of stress concentration. Failure is assumed to take place when the peak stress reaches the fatigue limit or the ultimate tensile strength of the material, as the case may be. The method to be discussed, then, is the method of calculating the appropriate factor of stress concentration.

The first step consists in determining the theoretical factor K_T. The second step consists in correcting the factor K_T for material size effect. The size-corrected factor is designated K_N, because the correction is made by means of a formula proposed by Neuber. The factor K_N constitutes the predicted value of the stress-concentration factor for fully reversed fatigue loading at stresses near the fatigue limit. For the prediction of ultimate (static) strength of a notched specimen, a third step is necessary: the factor K_N is corrected for plasticity effect and thus becomes the static notch strength factor K_u.

In the case of cracks, the root radius ρ is immeasurably small and consequently not known. It is therefore impossible to calculate a value of K_T; nevertheless, a value of K_N can be calculated, which is a major contribution of the theory of size effect. In this limiting case, the formula for K_N has an especially simple relation to the formula for K_T; the symbol K_{TN} is therefore used to denote the value of K_N for cracks ($\rho \rightarrow 0$).

In the following sections, the individual steps in the method are discussed in more detail, and size effects in general are briefly discussed.

Theoretical Factors of Stress Concentration

Theoretical factors of stress concentration K_T are derived by the theory of elasticity which assumes materials to be elastic, isotropic, and homogeneous. Reference 1 is a standard reference for theoretical factors. Formulas and nomograms excerpted from this book have been published in several places, such as reference 5. A comprehensive collection of formulas and graphs for practical use is given in reference 6. When a theoretical solution is not available for a specific configuration, photoelastic results may be used, since they are equivalent to theoretical solutions in principle.

There is currently a very strong interest in measuring and defining the static strength of sheet material containing sharp notches and cracks; as mentioned previously, a main objective of this paper is to deal with this problem. The most important theoretical factors needed for this application are given in appendix A.

Examination of the literature shows that theoretical factors for practical configurations are generally obtained by interpolating in some fashion between simple cases for which mathematical solutions are available. The accuracy of the theoretical factors is therefore questionable in most cases.

Size Effects

In the introduction it was stated that the stress-concentration factors of notches are modified by a "material size effect," and that there are also other size effects on strength. At present, three distinct types of size effect are generally recognized (under a variety of names):

(1) Metallurgical size effects

(2) Statistical size effects

(3) Material size effects

Metallurgical size effects arise from two main factors. The first one is the difference in the rates of cooling between a large and a small piece when cast metal solidifies or when a wrought metal is quenched in

heat treatment. The second factor is the difference in the amount of cold or hot work done, for instance, in processing an ingot into either a thick plate or a thin sheet.

The statistical size effect arises from the fact that failure in a practical material starts at a weak spot. A large piece of material contains more weak spots than a small piece; consequently, it is probable that the weakest spot in a large piece is worse than the weakest spot in a small piece.

The material size effect, as mentioned in the introduction, is usually ascribed to the fact that engineering metals are not homogeneous but have a structure composed of grains. It is not possible at present to give any detailed explanation of how the existence of a grain structure produces a size effect; it is possible only to make some general observations which hint at the reasons. One observation is that similar specimens of different sizes made from the same material are not truly similar (physically similar), because the grain size does not vary with the specimen size. Another observation is that the properties of engineering metals (alloys) such as modulus of elasticity and tensile strength are conventionally measured on a gross scale - that is, they are measured as averages over volumes of material containing extremely large numbers of grains. Measured on this scale, the material is usually fairly isotropic, whereas individual grains are known to be decidedly anisotropic in many cases. Whatever the detailed reasons may be, the result of the material size effect is that geometrically similar notched specimens show less and less notch effect as the absolute size of the specimen decreases.

The present paper will concern itself only with material size effect. Some brief comments are therefore desirable at this point with regard to interaction between material size effect on the one hand and metallurgical or statistical size effect on the other hand.

One facet of metallurgical size effect is that the strength may vary significantly across the thickness of a thick part. Obviously the problem of estimating the strength of a notched part becomes extremely complex in such cases, and nothing useful can be said in a few words. For the present paper, it will be assumed that metallurgical size effects resulting in nonuniform properties across the thickness are absent. Other metallurgical size effects, such as the difference between the tensile strengths or elongations of a thin sheet and a heavy plate, are assumed to be taken into account by using properties determined on appropriate specimens.

Statistical size effects depend on the volume of material involved. The method of correcting for material size effect proposed in the present paper involves the use of a Neuber constant ρ' which is determined and

verified by tests on specimens of various sizes. Consequently, the method may be considered to include automatically some allowance for statistical size effect. Whether this allowance is always adequate, only future research and experience can show. The excellent correlations obtained in tests of series of geometrically similar specimens made of steel (ref. 3) suggest that separate allowances for statistical size effects are not needed at the present state of the art of predicting the strength of notched parts. (Statistical considerations are, of course, the only method of approach known when strength comparisons are made, for instance, of the strengths of constant-section shafts of the same diameter and various lengths.)

It should be noted that the division of size effects into the three types listed is based simply on historical development, rather than on a logical system of classification. In other words, the terms metallurgical, statistical, and material size effect do not define clearly distinct types of size effect. The last two terms, in particular, tend to define the method of analytical approach rather than the physical phenomenon itself. Failure to recognize this state of affairs has sometimes resulted in confusion as evidenced in papers and discussions in engineering societies.

Approaches to Material Size Effects

Because the material size effect on notch strength is generally attributed to the existence of a grain structure, several authors have investigated the correlation between size effect and physical grain size of some specific materials. However, these approaches have not been developed into general prediction methods.

The method proposed by Neuber in reference 1, which forms the basis for the method of the present paper, does not consider the actual grain structure but introduces an idealized grain or "block" structure. This structure is a mathematical abstraction which has no known (direct) relation to the physically observable grain structure, except that the mathematical "grain" appears to be several times larger - perhaps one order of magnitude larger - than the physical grain size in steels. The mathematical theory of the stress distribution in the block structure assumes that the stress is uniform over each block. No detailed physical reasoning was advanced by Neuber (or any subsequent authors) as to why this block model of the material should give better results than the continuum model used in the conventional theory of elasticity. In essence, the block-model approach rests simply on the empirical observation that the smaller the notch radius, the more the experimental factor lies below the theoretical factor. The approach is thus strictly phenomenological.

Some authors have approached the problem by using as controlling parameter the volume of material which is stressed higher than, say, 95 percent of the peak stress. Other authors have used the stress gradient associated with the notch as a control parameter. These two approaches and the Neuber block approach are essentially equivalent; the choice between them is largely a matter of personal preference. This does not mean that the various published theories based on these approaches are identical, because additional assumptions are needed to formulate a complete theory; for instance, the 95-percent value quoted above may either be assumed to apply to all materials or it may be assumed to vary as a function of some material characteristics.

The stress-gradient approach may perhaps be regarded as preferable to the block approach because it permits a slightly more natural inclusion of the size effect on unnotched parts in bending, as a result of the linear stress distribution given by the elementary bending theory. However, as developed at present, the approach is more cumbersome for application to notched parts, which constitute a much larger problem in practice than unnotched parts.

[Calculation of K_N in dimensioned?]

Correction for Material Size Effect

The approach to the size-effect problem used by Neuber has been outlined in the preceding section. The correction for size effect proposed by Neuber in reference 1 consists essentially in the simple formula

$$K_N = 1 + \frac{K_T - 1}{1 + \frac{\pi}{\pi - \omega}\sqrt{\frac{\rho'}{\rho}}} \qquad (1)$$

where K_T is the theoretical factor of stress concentration as before, K_N is the factor corrected for size effect (hereafter termed "Neuber factor" as in ref. 3), ω is the flank angle (fig. 1(a)), ρ is the root radius of the notch, and ρ' is a material constant, called the Neuber constant in reference 3. In Neuber's derivation, ρ' represents the "radius" of the block which he postulates to be the fictitious building unit of the material.

The flank angle was introduced by Neuber into formula (1) on the basis of considerations separate from the consideration of the block concept. (It should be noted that in Neuber's scheme for estimating K_T values, the flank angle does not appear at all.) The analysis of fatigue-test data has led a number of investigators to the conclusion

that formula (1) exaggerates the effect of varying the flank angle in
the range from zero to about 2 radians (114°), where practically all
tests have been made. Some investigators therefore drop the flank-angle
term in formula (1) completely; that is, they set ω equal to 0 in
formula (1) regardless of the actual value of the angle. This procedure
is felt to be somewhat drastic; on the other hand, the available data
are inadequate to establish empirical factors. For the purposes of the
present paper, a compromise has been made by writing formula (1) in the
modified form

$$K_N = 1 + \frac{K_T - 1}{1 + \frac{\pi}{\pi - \omega_e} \sqrt{\frac{\rho'}{\rho}}} \qquad (1a)$$

where $\omega_e = \frac{1}{2} \omega$ for $\omega < 2$ radians.

When $\omega \to \pi$, the notch disappears, and consequently there is neither
notch effect nor material size effect. When ω becomes large, the
radius ρ is generally large, and the result is a notch factor so close
to unity that size-effect correction is unimportant. Consequently, no
attempt is made here to suggest a value for ω_e when $\omega > 2$ radians.

In reference 3 it was shown that the Neuber constant ρ' for steels
could be taken to be a function of the tensile strength of the material,
shown graphically as a curve of $\sqrt{\rho'}$ plotted against tensile strength.
In the present investigation it was found that two curves are required
for wrought aluminum alloys (fig. 2), one for alloys in T condition
(heat-treated) and one for alloys in O (annealed) or H (strain-
hardened) condition. Like the curve for steels given in reference 3,
the curves shown in figure 2 were obtained by a trial-and-error pro-
cedure based on the analysis of notch-fatigue data. It may be seen
that for heat-treated aluminum alloys, the quantity $\sqrt{\rho'}$ ranges from
about 0.5 to 0.12 in.$^{1/2}$; compared on the basis of equal strength-
density ratios, the quantity $\sqrt{\rho'}$ for heat-treated aluminum alloys
averages about three times the corresponding value for low-alloy steels
as given in reference 2.

The factor K_N constitutes the predicted value of the fatigue
factor for fully reversed loading at stresses near the fatigue limit.
It also serves as the basis for computing static strength factors,
which will be discussed later.

Sharp Notches and Cracks

When the notch radius ρ is small compared with the depth of the notch and the width of the net section, all formulas for theoretical factors may be written in the form

$$K_T \approx 1 + \frac{\text{Constant}}{\sqrt{\rho}}$$

which is often useful when dealing with sharp notches.

For U-notches and slots, the flank angle ω is zero. For such cases, substitution of the expression above into formula (1) yields in the limit, as ρ approaches zero,

$$\lim_{\rho \to 0} K_N \equiv K_{TN} = 1 + \frac{\text{Constant}}{\sqrt{\rho'}} \tag{2}$$

It will be noted that this expression is identical with the expression for K_T, except that ρ' has taken the place of ρ. The value of ρ' is finite except for perfectly brittle materials. Thus, if ρ is decreased indefinitely for a notch while the other dimensions remain fixed, the value of K_N given by formula (1) tends toward a finite limit (K_{TN}), as long as ρ' is finite, while the theoretical factor K_T tends toward infinity. Because the expressions for K_T and the limiting value of K_N are identical, the symbol K_{TN} has been chosen to denote the latter.

For cracks, the tip radius is indefinite but extremely small; microscopic observations suggest that it is well under 10^{-4} inch. Calculations for aluminum alloys show that for $\rho = 10^{-4}$ inch, the difference between K_{TN} and K_N is only a few percent. Thus, the use of K_{TN} for cracks is justified. The use of K_{TN} instead of K_N might also be acceptable for a notch with a very small radius, but the computational advantage gained by using K_{TN} instead of K_N is usually negligible.

Numerical examples for the computation of K_{TN} are included in appendix B.

Remarks on Effect of Size Variations

In order to demonstrate the large changes in factors which result from varying the size of a part, a set of calculated curves is shown in figure 3. The configuration assumed corresponds to figure 1(a) (sheet with 60° V-notches), with $\frac{d}{w} = 0.15$ and w either 1 inch or 36 inches. The material is assumed to have $\sigma_u = 68$ ksi, which results in $\sqrt{\rho'} = 0.145$ in.$^{1/2}$ according to figure 2. Figure 3 shows K_{TN}, curves of K_N, and, so far as possible, K_T. Two general observations may be made on this figure.

The first observation is that the relation between the Neuber factor and the theoretical factor is so tenuous that the theoretical factor K_T cannot be regarded as a directly useful quantity when the notch radius lies between the smallest value likely to be produced in a controlled manner (say 10^{-4} inch) and the largest value shown ($\rho = 0.1$ inch). The factor K_T approaches direct usefulness only when ρ becomes larger than 0.1 inch. Radii of this magnitude are encountered in actual parts of fair size; however, actual parts for small machinery and notched specimens used for materials testing generally have notch radii well below 0.1 inch.

The second observation concerns geometric similarity. Points such as A and A', or B and B', represent geometrically similar specimens. (The flank angle and the ratio d/w are identical for both curves. Thus, to find a point A' which represents a specimen geometrically similar to A, it is only necessary to find the point at which the radius ρ is 36 times larger than for point A.) It is obvious that there are great differences in the Neuber factors, in spite of geometric similarity; in fact, the range of factors for the 1-inch-wide specimens does not even overlap the range of factors for the 36-inch specimens. In the range of proportions where size effect is important, the law of mechanical similitude (geometrically similar structures behave similarly when subjected to the same stress) is invalid, and it is futile to search for nondimensional plotting parameters to simplify the relations as was sometimes done in the past by experimenters.

Finally, figure 3 indicates that fatigue factors can be very large if the specimen is large; for instance, for a specimen width of 36 inches and a notch radius of 0.001 inch, the predicted fatigue factor is about 17. The frequently heard statement that large fatigue factors cannot be realized physically is based on improper generalizations of test results obtained on small specimens.

Correction for Plasticity Effect [is discussed]

In the elastic range, the stress distribution in the vicinity of a notch shows characteristically a high peak at the bottom of the notch. As the load on a notched specimen is increased, the peak stress will eventually reach the yield value and will no longer be proportional to the load. With further increase in load, the stress distribution will become more and more uniform, and the factor of stress concentration will approach unity more and more closely as the plastic region extends.

For the case of a circular hole in an infinitely wide sheet, Stowell has given a simple formula (ref. 7) which corrects the theoretical (elastic) factor for the effect of plasticity. For application to other notch configurations, this formula was generalized in reference 8 to read

$$K_P = 1 + \left(K_T - 1\right)\frac{E_{s,p}}{E_{s,n}} \tag{3}$$

where K_P denotes the factor of stress concentration in the plastic range, $E_{s,p}$ the secant modulus corresponding to the peak stress, and $E_{s,n}$ the secant modulus corresponding to the net-section stress. For all practical applications, K_N should be substituted for K_T in formula (3) in order to take care of size effect; as written $\left(\text{with } K_T \text{ instead of } K_N\right)$ formula (3) is valid only for ideal material which is ideally brittle $\left(\rho' = 0\right)$.

In first approximation, a notched specimen may be assumed to fracture when the peak stress at the bottom of the notch becomes equal to the tensile ultimate stress. If the subscript u is used to designate values appropriate to this special case, the (size-corrected) equation (3) becomes

$$K_u = 1 + \left(K_N - 1\right)\frac{E_{s,u}}{E_{s,n}} \tag{4}$$

where $E_{s,u}$ is the secant modulus corresponding to the stress at the ultimate load of a simple tension specimen. In reference 4, values of $E_{s,u}$ were obtained from stress-strain curves. In general, complete stress-strain curves (up to failure) are not available, but the permanent elongation measured after failure is a property which is universally determined as a materials property. The modulus $E_{s,u}$ can be estimated from this elongation e by the formula

$$E_{s,u} = \frac{E}{1 + \dfrac{keE}{\sigma_u}} \tag{5}$$

where E is the elastic (Young's) modulus, while k is a factor some-
what less than unity which corrects for the fact that the elongation
measured after fracture includes some nonuniform elongation that takes
place after the maximum load ("ultimate load") is exceeded. For all
calculations shown in this paper, the value of 0.8 was used for k.

The use of formula (5) eliminates the need for a stress-strain
curve, provided the net-section stress is below the proportional limit
so that $E_{s,n} = E$ in equation (4). This condition is fulfilled in the
great majority of the tests discussed later in this paper; it may not
be fulfilled when the notch is a very short crack, or when a machined
notch is either very shallow or has a fairly large radius. In such
cases, with $E_{s,n}$ a variable, the direct use of equation (4) becomes
awkward because the solution must be effected by trial and error. To
avoid this difficulty, a curve of K_u against K_N can be computed for
a given stress-strain curve by solving equation (4) for K_N and assuming
a series of values for the net-section stress at failure. Some typical
curves of this nature are shown in figure 4. When K_u is sufficiently
large to keep the net-section stress below the limit of proportionality,
the curves are straight lines. For 7075-T6 sheet, the curve deviates
from the straight line for $K_N < 3$ but only slightly. For the 2024 alloy,
however, the straight-line portions of the curves begin near or beyond the
right-hand border of figure 4.

Secondary Corrections

The corrections of the stress-concentration factor for material
size effect and for plasticity effect are generally the most important
ones. However, two other corrections may be sufficiently important to
require application in some cases. Both are entirely empirical and
based on very meager data; they should therefore be regarded as stopgap
formulas subject to improvement either by theory or by analysis of more
extensive sets of data when they become available. The two corrections
are a "flow-restraint" correction and a buckling correction.

The theoretical factor of stress concentration is the ratio of peak
stress to average stress over the net section; this factor is, by its
nature, always larger than unity. The experimental factor for ultimate
strength can be defined as the ratio of ultimate stress of the material,
measured on specimens without notches, to net-section stress at failure

of the notched specimen. (It is presumed here that conventional engineering methods are used, that is, the load used for computing the stress is the maximum load developed in the test and the area used is that measured before the test begins.)

It has been known for decades that the experimental ultimate-strength factor for ductile materials can be substantially less than unity. In the face of the fact that a stress-concentration factor must be larger than unity, this observation can be explained only by the assumption that material at a notched section may develop a higher strength than a specimen devoid of notches. The increase in strength is attributed to restraint against flow of the metal in the notch region, exerted by the material in the adjacent regions which are under a lower stress.

Although a large amount of research has been devoted to the problems of fracture, particularly under conditions of restrained flow, there is little or no information for practical design use. In order to round out this paper, an empirical formula has been devised which has given reasonable accuracy in predicting the tensile strength of notched sheet specimens. (The formula is not applicable if the cross section of the specimen approaches a square or circle.) It consists of a correction factor applied to the factor K_u given by formula (4) and results in the corrected factor

$$K_u{}^* = \frac{K_u}{1 + B \frac{\sigma_y}{\sigma_u} \tanh \frac{\rho}{\rho'}} \tag{6}$$

where B is a function of K_T given by the graph in figure 5. It may be noted that the correction is most important for rather mild notches, having a maximum value at $K_T \approx 3$. For very sharp notches or cracks, on the one hand, or very mild notches on the other hand, it becomes negligible.

The second, or buckling, correction applies to sheet tension specimens containing an internal transverse slot or crack, such as shown in figure 1(b). Examination of the stresses in such a specimen shows that there are compressive stresses in the transverse direction, approximately parallel to and close to the boundaries of the slot. If the sheet is thin, these compressive stresses cause buckling of the lips of the slot out of the original plane of the sheet and thus cause stresses which add to those due to the stress-raising action of the slot in the unbuckled sheet. If desired, these additional stresses due to buckling can be eliminated in tests by using guide plates on both sides of the sheet. The use of such guide plates is fairly standard

16

practice in fatigue tests, but has not been general practice in (static) tensile tests. When no guide plates are used, a correction should be made for the buckling effect.

Since the distribution of the stresses around the slot is highly nonuniform, a theory for the buckling stress would be rather difficult to derive, and the theory for the stresses arising from the postbuckling deformation would be even more difficult. No attempt appears to have been made to develop such a theory. Experimental evidence has shown that the buckling effect is important only in rather extreme cases - thin sheets with long slots or cracks. Consequently, it is felt that as an interim measure, a simple empirical correction may be regarded as acceptable. The correction is incorporated in the formula

$$S_u{}^* = S_u\left(1 - 0.001\,\frac{2a}{t}\right) \tag{7}$$

where $S_u{}^*$ denotes the predicted net-section failing stress when buckling is not prevented, while S_u denotes the predicted stress when buckling is prevented. $\left(S_u \text{ equals } \sigma_u/K_u \text{ or } \sigma_u/K_u{}^*, \text{ but the latter case is unlikely to occur in practice.}\right)$

EXPERIMENTAL EVIDENCE

General Discussion

The methods of predicting fatigue and static notch factors presented in this paper rest on a theory of size effect. This theory is an "engineering" or "working" theory, terms which are meant to imply that no claim is made for great depth of the physical foundations. As a matter of principle, a theory of this type should be substantiated by a volume of test data commensurate with the scope claimed for the theory - a principle unfortunately often violated in the literature. In an attempt to honor this principle, a rather large set of comparisons between test results and predictions is presented in the following sections.

In some types of tests, it is possible to achieve test accuracies of a few percent and to demonstrate that the repeatability of the tests is of the same order. In such circumstances, differences between theory and tests which amount to, say, 20 percent can and must be attributed essentially to weakness of the theory. However, in the field of notch strength (fatigue or static), the test accuracy and repeatability are not within a few percent at present. While there has been a vast amount of discussion on the subject of scatter in fatigue life, there has been

almost no discussion of scatter in fatigue <u>factors</u>. As a result, some investigators tend to consider fatigue factors as very precisely established values; some effort has therefore been made in the follwing discussions to point out test evidence which shows that the precision and repeatability of experimental fatigue factors (and also of static notch factors) are not very high at present. Anticipating the more detailed discussions, it may be stated here that test errors in the general sense (including inadequate sample size) may well contribute about as much to differences between test and prediction as weaknesses of the prediction method.

L
1
7
4
3

Fatigue Factors

The usefulness of formula (1) for computing fatigue factors for low-alloy steels was shown in reference 3. In particular, this reference shows several series of tests which demonstrate very directly and convincingly the ability of the formula to predict the effect of size variations on geometrically similar specimens. The discussion on the prediction of fatigue factors for aluminum alloys in the present paper is therefore less extensive.

A proper assessment of the accuracy of prediction can be made only in the light of adequate awareness of possible test errors. Consequently, one section will discuss some sets of tests which indicate directly - that is, without reference to predictions - the magnitude of possible test inaccuracies; comparisons between tests and predictions are given only in a cursory manner in this section. Another section will give a comprehensive discussion of comparisons between tests and predictions for all the available data.

<u>Accuracy and adequacy of fatigue test data.-</u> The test data utilized in this investigation were obtained from references 9 to 33.

The accuracy and adequacy of fatigue test data depend on the following main items:

(1) Minimization of errors in the measurements of specimen dimensions and test loads

(2) Minimization of stresses due to eccentricities and machine vibrations

(3) Minimization of surface stresses due to machining and polishing

(4) Testing of a sufficiently large number of specimens to obtain a good statistical average

Other items that may require attention are corrosion effects and proper control of heat treatment. With regard to the measurement of specimen dimensions, it should be remarked that specifying narrow tolerances for small notch radii on the drawing is not a substitute for measuring these radii, as some experimenters trustingly assume.

It is beyond the scope of this paper to discuss these test problems in detail. However, detail plots of some test data will be shown to give indications of possible test inaccuracies.

Figure 6 gives plots of K_F values derived from tabulated fatigue data in references 10(a) and 10(b). The following observations may be made with regard to this figure:

(1) At $N = 10^8$ cycles, two alloys show differences of 16 percent and 25 percent, respectively, between the 1951 and the 1955 data. Both alloys were well established and tested before 1951; it may be supposed, therefore, that the differences reflect mainly uncertainties in fairing the S-N curves rather than differences in the curves brought about by the addition of extensive new test data. (If this supposition were disproved, one would be forced to the even more dismaying conclusion that fatigue data more than 4 years old should not be used.)

(2) For two of the alloys shown in figure 6, the value of K_F at $N = 10^7$ is 20 to 25 percent higher than at $N = 5 \times 10^8$, the nominal fatigue limit. Now, it appears to be at least tacitly agreed among fatigue engineers that the fatigue factor is a single-valued function of the stress level. If this point of view is accepted, then it must be concluded that the curve of K_F against cycle number should rise monotonically toward a maximum at the fatigue limit. A maximum at a lower number of cycles must then be interpreted as resulting from inaccurate determination of the basic S-N curves (plain and notched).

Thus, the data shown in figure 6 suggest from two different considerations (differences between 1951 and 1955 values; shapes of curves) that two K_F values determined under nominally (or essentially) identical conditions may differ from each other by 15 to 25 percent.

The predicted factors K_N are shown in figure 6 as horizontal lines beginning at the fatigue limit ($N = 5 \times 10^8$). The agreement with the experimental values is satisfactory except for 2024-T4 alloy.

Figure 7 shows experimental and calculated factors for two series of tests on British alloys (ref. 32). In all tests the notch configuration was the same except for the flank angle, which is given by the abscissa scale. For D.T.D.683 (similar to 7075-T6, naturally aged,

extruded), the agreement between test and calculation is satisfactory, the largest difference being 14 percent. For B.S.S.6L1, on the other hand, the test points are consistently higher than the predictions (on the average about 17 percent). In the absence of evidence to the contrary, this systematic difference can only be charged to weakness of the prediction method. In addition, the point at $\omega = 30^{\circ}$ is apparently out of line. This error, which is about 20 percent, must presumably be charged to test error.

Very instructive - and dismaying - is a study of two investigations of size effect on rotating beams. The first investigation (ref. 15) showed a trend opposite to the trend generally observed: the fatigue factor decreased with increasing size of the specimens. In an attempt to clear up this anomaly, another investigation was undertaken (ref. 16), in which the specimen configurations of the first investigation were duplicated insofar as practicable, changes being made only so far as necessary to accommodate the testing machines available in the second laboratory.

Figure 8(a) shows the fatigue factors K_F obtained. Circles denote the factors reported from the first investigation. Factors obtained in the second investigation are shown as bars, as reported by the investigators, based on their estimates of uncertainties of determination. Also shown is the curve of factors K_N calculated by the present procedure. The following two observations may be made on figure 8(a).

(1) The agreement between the results of the two investigations is reasonable for the largest test specimens $\left(1 \text{ inch and } 1\frac{3}{4} \text{ inches}\right)$. It deteriorates as the specimens become smaller; for the smallest specimens, one laboratory gives a factor K_F about 50 percent higher than the other laboratory.

(2) The uncertainty band estimated by the second group of investigators is about ±17 percent.

Figure 8(b) shows the fatigue limits (unnotched and notched) from which the fatigue factors shown in figure 8(a) were derived. Again, the agreement is either reasonable, or quite good, for the two largest sizes. There is also rather good agreement for the smallest sizes of the notched configuration, but a large disagreement for the smallest unnotched specimens. For the 1/4- and 1/2-inch specimens - which bracket the usual range of rotating-beam sizes - the agreement is very poor, with differences up to 30 percent.

The examples shown were culled from published data. They indicate clearly that the accuracy and repeatability of fatigue data currently available from the literature are rather poor. Obvious test errors larger than 20 percent can occur in one out of six sets of tests run concurrently in one laboratory, and repeat tests in a different laboratory can show differences of the same order or larger.

Accuracy of prediction of fatigue factors.- Reference 9 is a survey of work done over a period of more than two decades by the research laboratories of the Aluminum Company of America to study and establish the properties of alloys produced by this company. It constitutes an unusually cohesive set of data, having been obtained in one laboratory under the same direction for the entire time. The data on tensile strengths and on fatigue limits for unnotched and notched specimens presented in figure 2 of reference 9 were therefore used as the main basis for establishing the curve of $\sqrt{\rho'}$ versus σ_u shown in figure 2 of the present paper. The specimens used in these fatigue tests were rotating beams with a 60° V-notch having a root radius of 0.0002 inch and a K_T value of about 19.

Figure 9 shows experimental values of K_F (symbols), determined from the data given in figure 2 of reference 9, and curves of K_N computed by using figure 2 of the present paper. Since ρ' was established essentially by fitting these data, figure 9 shows only the quality of the fit obtained on the base data. The largest difference between experimental and predicted factors occurs at $\sigma_u = 68$ ksi for 2024-T3 alloy, with the predicted factor 20 percent higher than the experimental factor. The next largest difference is 10 percent.

Figure 10, consisting of six plots, constitutes a summary of comparisons between experimental factors K_F and computed factors K_N for fatigue data contained in references 10 to 33. The plots show the relation between the ratio K_N/K_F (ratio of calculated to experimental factor) and the notch radius. This type of plot, used first in reference 3, gives a picture of the overall agreement between experimental and predicted results. The notch radius, rather than the theoretical factor K_T, was chosen as parameter for the comparison plots because the accuracy of the machined radius obviously becomes more questionable as the radius becomes smaller, and consequently more disagreement between calculation and experimental results may be expected for small radii. In order to aid in the appraisal of the plots, scatter bands of ± 10 percent and ± 20 percent have been indicated. More detailed information is given in table I.

An explanation is appropriate with regard to the K_N/K_F ratios for D.T.D.646B alloy listed in table I(e). It will be noted that the numbers tabulated are not simply the ratios K_N/K_F, but $K_N/1.35K_F$. The authors of reference 31 discuss the fact that the specimens which they used to determine the plain (unnotched) fatigue limit were, in fact, not plain; a parallel-sided central portion was joined to wider end portions by fillets. The stress-concentration factor for these specimens was calculated to be 1.35 by the authors of reference 31.

Table II gives a summary of the comparisons shown in tables I(a) to I(d) and figures 10(a) to 10(d), that is, for 2024 and 7075 alloy. The average value of the ratio K_N/K_F ranges from 1.00 to 1.09 and indicates a reasonably close overall agreement that tends to be slightly conservative, a result which was aimed at in deciding on the curves of $\sqrt{\rho'}$ versus σ_u. For the axial-load tests on either 2024 or 7075 alloy, only 15 percent of the points fall outside the ± 20 percent scatter band. For the rotating-beam tests, the percentage falling outside the ± 20 percent band increases to nearly 30 percent for the 7075 alloy and to 50 percent for the 2024 alloy. The last group is somewhat disappointing; however, it is the smallest group (12 points, against 24 to 56 for the other three groups). Moreover, the highest as well as the two lowest values of K_N/K_F are based on data from the same laboratory, an observation which suggests the possibility of inadequate test data.

On the basis of the data analyzed in this paper, then, it may be said that the chance of a prediction error being larger than 20 percent is about 1 in 5 for axially loaded parts and somewhat larger for rotating beams. The chance of a test error being larger than 20 percent cannot be estimated because of paucity of data; however, the discussion in the preceding section suggests that this chance is not very much less than 1 in 5. Thus, it may be said that the accuracy of prediction is probably only slightly inferior to the accuracy of the data currently available.

Critique of method for predicting fatigue factors.- The prediction method presented employs a material constant ρ' which was derived from the currently available test data. Thus, the method is, in principle, simply a correlation of available test data on the basis of a rather crude mathematical model which expresses size effect.

Under these circumstances, the accuracy of the prediction method can be, at best, only equal to the accuracy of the test data available. The prediction method in its present form apparently falls somewhat short of this best possible accuracy. Some improvement of the accuracy of prediction might be achieved by a more searching analysis, possibly by some modification of the method. An improvement approaching an order of magnitude, however (say a reduction of prediction errors from

20 percent to 3 percent), would not be possible unless and until the accuracy of the test data available is improved by about an order of magnitude by increasing the number of tests by at least one order of magnitude. Before such large test series are initiated, it would be well to study the effects of some variables - in particular, surface stresses due to machining and polishing - more carefully than has been done heretofore. With better knowledge of such effects, the prediction accuracy might be improved by introducing suitable correction factors.

The use of Neuber's unit-block concept, which leads to formula (1), is only one of a number of approaches to the problem of size effect. Some authors have suggested the use of the stress gradient at the point of peak stress as a parameter for correlation. The stress-gradient approach and the unit-block approach are obviously closely related in principle. The former appears to offer some advantages and some disadvantages over the latter, but so far, it has apparently not been developed into a method of reasonable scope. Studies on the basis of stress gradient should lead to a better knowledge of size effect in bending, encountered for instance in rotating beams (without notches). A study of this last item is also highly desirable for better evaluation of fatigue factors derived from rotating-beam tests.

Static Notch Factors

The evidence on static notch factors presented herein, consisting of experimental factors and corresponding predicted factors, is divided into two groups. The first group consists of specimens containing actual or simulated cracks; the information on this group is presented in the form of plots (figs. 11 to 13) and is discussed in some detail because there is currently a strong interest in the problem of strength of cracked parts. The second group consists of specimens with machined notches; information on this group is presented in tabular form only (table III) and is discussed only briefly.

All the static notch factors were obtained for this paper by using the maximum load carried by the specimen, divided by the net area existing before the test load was applied.

Sources of data.- The experimental evidence was obtained from references 4, 22, 23, 24, 27, 34, 35, and 36. Also included are some unpublished NASA and Lockheed data. Almost half the data on sheet specimens with simulated cracks are unpublished data from the Lockheed Aircraft Corporation, California Division. The courtesy of the Lockheed Corporation in granting permission to present these data is gratefully acknowledged. These data will hereafter be designated as Lockheed data.

Materials properties used in calculations.- For the calculation of
fatigue factors, it is necessary to know only the tensile strength of
the material; even this property enters into the calculation only indi-
rectly (to determine ρ'), and the calculation is not sensitive to nor-
mal variations of the strength value. For the calculation of static
notch strength on the other hand, it is necessary to know tensile
strength, modulus, and elongation (or stress-strain curve), and the cal-
culation may be fairly sensitive to changes in these quantities. The
materials properties used in the calculations therefore require some
discussion.

For the research purpose of demonstrating the accuracy of the pro-
posed method, it would be desirable to use actual material properties
as determined by coupon tests. Actual material properties were conse-
quently used for plate specimens, bar specimens, and the narrowest sheet
specimens, $w = 2\frac{1}{4}$ inches (with edge notches).

Preliminary calculations for all sheet specimens wider than $2\frac{1}{4}$ inches
with internal notches (cracks or saw cuts) were based on typical material
properties taken from reference 37 because only a limited number of
coupon data were available. These calculations showed a number of very
unconservative strength predictions for 7075 sheet specimens; inspection
of the test data indicated large scatter in some test series. The num-
ber and magnitude of the prediction errors on the unconservative side
were considered objectionable in view of the potential use of the method
for calculating the strength of damaged structures in accordance with
airworthiness requirements. A reasonably rational modification of the
method was therefore sought which would substantially reduce the number
of definitely unconservative predictions. The modification employed
for the final calculations was the use of minimum rather than typical
elongation for 7075 sheet specimens except the $2\frac{1}{4}$ - inch-wide edge-notch
specimens.

Calculations for clad material were made as follows: The factor
K_u was calculated by using the properties of the core material; this
factor was then divided into the tensile strength of the clad material
to obtain the net-section stress, and finally the buckling correction
was applied. The material properties are given on each plot in fig-
ures 11 to 13.

Special features of specimens with cracks.- Several special fea-
tures of the specimens with cracks and of the presentation of the data
obtained on some series deserve some discussion.

The NASA (NACA) specimens contained large circular holes as initial stress raisers to produce fatigue cracks; the static tests under discussion here thus deal with hole-plus-crack configurations. It is well known that the stress-concentration factor of such a configuration is the same as that of a crack-alone configuration with the same tip-to-tip length, provided that this tip-to-tip length is substantially larger than the diameter of the hole. For configurations of holes with short cracks, no theory has been developed. A rough estimate was therefore made of the region in which a hole-plus-crack configuration might be expected to differ from a crack-alone configuration, and this region is shown in figures 11 and 13 as a stippled area. Only a few test points lie in or close to this region.

A feature common to the majority of the specimens is the simulation of cracks by jeweler's saw cuts 0.008 to 0.013 inch wide. A few early tests made in various laboratories had indicated that in aluminum-alloy sheet, such a saw cut gave about the same result as a fatigue crack of the same length. When tests were made in larger numbers, however, it became apparent that a difference between cracks and saw cuts can be found, although it may be obscured by test scatter.

As far as computation is concerned, the saw cut poses the difficulty of an indefinite geometry at the corners. If the corners were truly sharp (zero radius), the theoretical factor of stress concentration would be infinite, and the factor K_u would be the same as for a crack. However, since the saw teeth are not infinitely sharp, the corners of the cut will be rounded off somewhat. In view of these considerations, it was decided to show two computed curves for all test series with saw cuts. For one curve, the notch configuration is assumed to be a crack with zero tip radius. For the other curve, the notch configuration is assumed to be a slot with a semicircular end (tip radius equal to one-half the width of the saw cut).

The Lockheed tests of specimens 20 inches wide (fig. 11(b), lower part) and of some of the specimens 9 inches wide (fig. 11(c), lower part, and fig. 11(d), upper left) were made for two thicknesses, in both grain directions (longitudinal and transverse), and were made in duplicate. The test results were pooled for each width; thus, each test point represents the average of eight tests, while the tick marks on the vertical bars show the highest and the lowest test value.

Finally, some explanation of the edge-notched specimens shown in figure 11(e) seems desirable. When the basic specimens with simicircular edge notches were subjected to fatigue loading, cracking took place in all cases only on one side. On a specimen with a crack on one side only, the line of action of the force applied by the grips would not pass through the center of the net section, and the formulas for symmetrical notches would not be applicable. In order to make these formulas

applicable, the specimens were "symmetrized" either by removing material (right-hand sketch) or by making a saw cut of the same depth as the crack on the opposite side of the specimen (center sketch).

In a few tests, buckling at the edges of an internal crack or saw cut was prevented by guide plates. These tests are referred to as "guided" and are indicated by special symbols.

Results and discussion of specimens with cracks.- The results for specimens with cracks are shown in figures 11 to 13 arranged in the following order:

(1) Sheet specimens, arranged in decreasing order of width (fig. 11)

(2) Plate specimens (fig. 12)

(3) Bar specimens (fig. 13)

Sheet specimens are of two types: with internal cracks (figs. 11(a) to 11(d)) and with edge cracks (fig. 11(e)).

The tests on sheet specimens (fig. 11) constitute the largest part of the data. As mentioned previously, calculations were based on typical properties (with the exception of the NASA test on 5052-H34 and the NASA tests on specimens with edge notches). The comparison between tests and calculations thus affords an index of the accuracy with which the strength of an actual production structure would be predicted by a structural designer. On the other hand, the data are not very suitable for discussing in any detail the "resolution power" of the theory and possible improvements; these questions will be discussed briefly under the heading "Critique of method for predicting static notch strength."

Inspection of all parts of figure 11 indicates that the goal of a slightly conservative method of prediction has been achieved reasonably well if $\rho = 0$ is used. Unconservative predictions are largely confined to the 9-inch specimens of clad 2024-T3 (fig. 11(c), lower left), for which the data show large scatter and are open to some doubt.

Attention is called to the fact that a generally conservative prediction was achieved for 7075-T6 by using minimum rather than typical elongation. As a result, some predictions for this material are quite conservative (12-inch specimens, fig. 11(c), upper right). The point at $\frac{2a}{w} = 0.26$ in this figure suggests the scatter that may be experienced in data for this material, being obviously much higher than the points to either side of it.

In the figures pertaining to tests with saw cuts, it may be observed that the difference between the calculated curve for cracks ($\rho = 0$) and that for slots (ρ = one-half width of saw cut) is negligible for 6061-T4, the most ductile material (fig. 11(d)), becomes significant for 2024-T3, and becomes quite large for 7075-T6.

In figure 11(e) it may be observed that test results for saw cuts (circle symbols) lie entirely (for 2024-T3) or largely (for 7075-T6) on the upper edge of the scatter band formed by cracked specimens. Thus, there is a significant difference between cracks and saw cuts. In addition, it may be noted that the calculation for the slot configuration is still somewhat conservative as the upper limit for the sawcuts. However, for wide specimens (35, 30, and 20 inches, figs. 11(a) and 11(b)), the calculation of saw cuts as slots is unconservative. From these observations, the conclusion may be drawn that jeweler's saw cuts should always be calculated as cracks if a conservative prediction is desired. On the other hand, test results as high as those predicted by a slot calculation should not be a cause for surprise.

Recent research indicates that the static strength of specimens with fatigue cracks is influenced by the magnitude of the fatigue stress at which the crack was generated. However, results in this area are too few to justify discussion here other than to call attention to the fact that in future tests the fatigue stress should be recorded; the best test practice is to complete the fatigue test at the lowest theory level.

For 2024-T3 and 7075-T6, a wide range of specimen geometry is covered in the tests shown. The results show that the thoery deals adequately with the effects of geometry over the range covered. They also indicate that the simple adaptation of the method to clad materials is satisfactory for these materials.

Concerning the ability of the theory to deal adequately with a wide range of ultimate strength and elongation, the evidence available at present is rather limited. Results for sheet materials other than 2024-T3 and 7075-T6 are shown in figure 11(d). For clad 2024-T81, the prediction is somewhat conservative, but may be considered acceptable because the calculated slot curve agrees closely with the average test points. For 5052-H34, the prediction for the Lockheed tests (upper right of fig. 11(d)) is very conservative (based on typical properties). Check tests were therefore made at the NASA Langley Research Center (lower right). For these tests, actual material properties were determined, and the uncertainty about notch configuration was eliminated by terminating the saw cuts with semicircles, produced by drawing nylon threads impregnated with abrasive repeatedly over the ends of the cut. The agreement between experimental and calculated results is better, on the average, for these check tests than for the original tests.

For the 6061-T4 material (fig. 11(d), lower left), the predictions are extremely conservative. Circumstantial evidence suggests the possibility that the actual tensile strength may have been substantially higher than the typical value used in the calculation. If this possibility is discounted, then the method of prediction becomes suspect. A general study of comparisons between tests and predictions (including materials other than aluminum alloys) suggests that the method may become excessively conservative for highly ductile materials. Formula (5) suggests that ductility might be measured for this purpose by the quantity eE/σ_u (in effect, the ratio of elastic modulus to secant modulus for ultimate strength). For 6061-T4 material, this quantity is 63, while for the other aluminum alloys covered by this investigation, the quantity ranges from 14 to 36. Thus, by this criterion, 6061-T4 material represents an extreme case of high ductility. Evidence on other extreme cases suggests that formula (4) might be improved by a modification: the modulus $E_{s,n}$ should perhaps be based not on the net-section stress, but on some stress intermediate between the net-section stress and the gross-section stress. Available test evidence is too scanty and too uncertain, however, to do more than suggest that a modification might be appropriate.

The plate specimens (fig. 12) were made from 1-inch-thick plate, machined down to 0.25 inch at the test section. The agreement with the calculations (based on actual properties) is satisfactory for all four materials, the predictions tending to be slightly conservative.

The bar specimens (fig. 13) were 0.75 inch thick and thus represent the largest thickness tested. For 2024-T4, the prediction is again slightly conservative. For 7075-T6, however, the prediction is somewhat unconservative, in spite of the fact that the calculation was based on the listed minimum elongation (7 percent) instead of the actual elongation of 10.8 percent. This test series, then, suggests that thickness effects (variation of stress through thickness and attendant biaxiality effects on material) may become significant for the proportions of these specimens.

Overall conclusions may be drawn as follows for specimens with cracks:

(1) Predictions tending to be slightly conservative may be expected for thicknesses up to somewhat less than 3/4 inch. For larger thicknesses, the predictions may become unconservative.

(2) The predictions appear to be very conservative for highly ductile materials $\left(eE/\sigma_u > 50\right)$.

(3) For materials which exhibit appreciable scatter, it may be necessary to make an allowance for scatter if the number of unconservative

predictions is to be minimized. For 7075 alloy, this allowance can be made by using minimum elongation in the calculation.

Although saw cuts have been used as laboratory substitutes for cracks, they should not occur in actual structures; consequently, the question of predicting the strength of parts with saw cuts in rather academic. The tests indicate that bracketing calculations may be made by assuming the cut to act either as a crack or as a slot (with semicircular ends).

Results for specimens with machined notches.- Results for specimens with machined notches are presented in table III. It will be noted that a very wide range of notch acuteness is covered, in that K_T varies from 1.5 to 38. Calculations were based on actual properties, except that for 7075-T6 the minimum elongation as listed in reference 37 was used.

Inspection of the tables shows that for more than 75 percent of the tests, the prediction error is not more than 5 percent. Nominally identical specimens with 60° V-notches show ratios of calculated to experimental factors K_u ranging from 0.93 to 0.96 for the 2024-T3 material, and ratios ranging from 0.88 to 1.00 for the 7075-T6 material. Thus, for the latter material, the accuracy of prediction appears to be determined mostly by scatter of the material properties. For 2024-T3 material, on the other hand, prediction errors apparently should be attributed more to the prediction method than to material scatter.

Critique of method for predicting static notch strength.- The agreement between prediction and test for the rather large volume of data presented indicates that the strength-prediction method offered has merit for engineering use. However, the test data available are not as extensive in some respects as might be desired. It seems appropriate, therefore, to discuss a number of considerations, partly to help in evaluating the method, partly - and more importantly - to indicate research which seems desirable to either confirm the method or modify it.

In the calculation of the net-section stress and of the factor of stress concentration, use is made of the initial notch configuration which exists before loading is started, and the maximum load carried by the specimen is considered to be the failing load. This procedure disregards the observed fact that in some materials, a slow extension of the crack begins at a load measurably below the maximum load; thus, the geometry of the part at the instant of failure (i.e., complete fracture) is not the geometry assumed in the calculation. From the physical point of view, this must be regarded as a weakness of the method, and it is possible that elimination of this weakness may result in improvement of the strength predictions. It should be emphasized, however, that any procedure which involves measuring the actual crack length at the instant of failure is a testing procedure, not a prediction procedure;

a prediction procedure must logically be based entirely on knowledge which is available <u>before the loading begins</u>.

Intuitively, one may assume that fracture behavior is associated with ductility, which is measured most often by elongation on a rather large gage length, a 2-inch gage length being probably the most common one. However, fracture begins as a crack of microscopic or submicroscopic width. It may be, therefore, that elongation values based on a very small or zero gage length are a better basis for fracture calculations; reduction in area might be considered as a measure of elongation with zero gage length. To serve as a basis for calculations on sheet specimens, the reduction of area should be measured on sheet specimens. Such measurements have not been widely made in the past; consequently, it was not possible to examine the merit of this idea on the basis of available data.

As mentioned under the heading "Materials properties used in calculations," minimum rather than typical elongation values were used for 7075 alloy. This modification of procedure might be regarded as a special allowance for elongation values of 7075 alloy, which shows more scatter than 2024 alloys. However, there is at present no proof that scatter in elongation is indeed the main reason for scatter in notch strength. Some investigation of this question would be desirable.

The factor k in formula (5) is intended nominally to convert from total to uniform elongation. The value of $k = 0.8$ used in all calculations for this paper is a rounded-off average for the 2024-T3, 2024-T4, and 7075-T6 material used in the NASA tests. The use of this value for other alloys constitutes a simplifying assumption; it is possible that future research paying specific attention to this point might result in an improvement of the prediction method by introducing either the uniform elongation or a variable factor k.

With regard to the use of equation (4), two questions appear to be in need of investigation. Equation (4) represents the application of equation (3) to the special case in which the load is sufficiently high to cause failure. Equation (3) is a generalization of the theory developed by Stowell on the assumption that the plastic strains are small (of the same order as the elastic strains). In a specimen made of ductile material, the plastic strains at failure are an order of magnitude larger than the elastic strains. Consequently, the accuracy of Stowell's theory for describing conditions near failure might be questioned. It is well known, for instance, that a notch radius may be increased substantially in the process of loading before failure takes place.

The second question regarding equation (4) (or eq. (3)) concerns the use of the modulus $E_{s,n}$, the secant modulus corresponding to the

net-section stress. Stowell's derivation was for a hole in a sheet of infinite width; in such a case, net-section stress and gross-section stress are equal, and Stowell actually defined the reference stress as the stress at a large distance from the hole. The use of the net-section stress in equations (3) and (4) thus represents an interpretation of Stowell's theory for conditions not covered by the theory. The use of this interpretation is based on the fact that it has given good correlation with the great majority of the test results available. However, for some tests of highly ductile materials (especially mild steels), the predictions have been unduly conservative. Examination of the calculations for these cases suggests that the secant modulus in question should perhaps be based not on the net-section stress, but on some stress intermediate between the net-section and the gross-section stress.

Finally, the theoretical factors of stress concentration should be refined in some cases. The most commonly used formulas for the theoretical factors are valid only when the length of the notch (or slot or crack) is substantially greater than the thickness of the material. When the length of the notch is less than the thickness of the material, some attention should be given to the fact that the stress varies across the thickness. This situation is most likely to arise in practice when the absolute thickness of the material is large, which brings in the additional complication of differences in material properties due to metallurgical effects. Finally, directional effects may be significant, for instance, in forgings. It is clear, therefore, that the prediction method should not be applied blindly in these unexplored areas, and that additional checks and development of the method are highly desirable.

CONCLUDING REMARKS

A method is presented in this paper by means of which fatigue notch factors and static notch factors can be predicted for parts made of wrought aluminum alloys. Probable limitations and desirable improvements of the method are pointed out. The first part of the method (prediction of fatigue factors) has been applied previously to low-alloy steels. Preliminary explorations indicate that the second part of the method (prediction of static notch or crack strength) should be useful for steels and titanium alloys. A correlation of fatigue and static notch strengths, however, for steels or titanium alloys does not appear to be feasible at present.

Langley Research Center,
National Aeronautics and Space Administration,
Langley Air Force Base, Va., February 27, 1962.

APPENDIX A

THEORETICAL FACTORS OF STRESS CONCENTRATION FOR

SHEET SPECIMENS IN TENSION

The notch configurations used for notch tests on sheet material comprise external and internal notches (fig. 1).

For an external notch (edge V-notch as in fig. 1(a)), the procedure given in reference 1 is as follows:

(1) Obtain a shallow-notch factor K_S by means of the formula

$$K_S = 1 + 2 \sqrt{\frac{d}{\rho}} \tag{8}$$

(2) Obtain a deep-notch factor K_D by use of formula (69), chapter IV of reference 1. For convenience, this factor is given graphically in figure 14 for values of c/ρ up to about 9. For values of c/ρ beyond the limits of the graph, the asymptotic limit expression valid for large values of c/ρ may be used:

$$K_D = \frac{4}{\pi} \sqrt{\frac{c}{\rho}} \tag{9}$$

(Note that at the limit of the graph, the error due to using eq. (9) would be slightly over 2 percent.)

(3) Combine K_S and K_D into the final theoretical factor by means of the formula

$$K_T = 1 + \frac{\left(K_S - 1\right)\left(K_D - 1\right)}{\sqrt{\left(K_S - 1\right)^2 + \left(K_K - 1\right)^2}} \tag{10}$$

For an internal notch, assumed to be an ellipse (fig. 1(b)), the following procedure was used in reference 4 and is adopted here:

(1) The theoretical factor K_C for a circular hole with a diameter equal to $2a$ in a sheet of width w is found. Figure 15 gives K_C in graphical form.

32

(2) The theoretical factor for the elliptical hole is assumed to be given by the expression

$$K_T = 1 + \left(K_C - 1\right)\sqrt{\frac{a}{\rho}} \qquad (11)$$

For a transverse crack of length 2a, application of formulas (2) and (11) gives

$$K_{TN} = 1 + \left(K_C - 1\right)\sqrt{\frac{a}{\rho'}} \qquad (12)$$

APPENDIX B

NUMERICAL EXAMPLES

For all numerical examples, the material is assumed to be 2024-T3, with σ_u = 70 ksi and σ_y = 50 ksi.

Fatigue Factor

The fatigue factor is computed for the specimen shown in the following sketch:
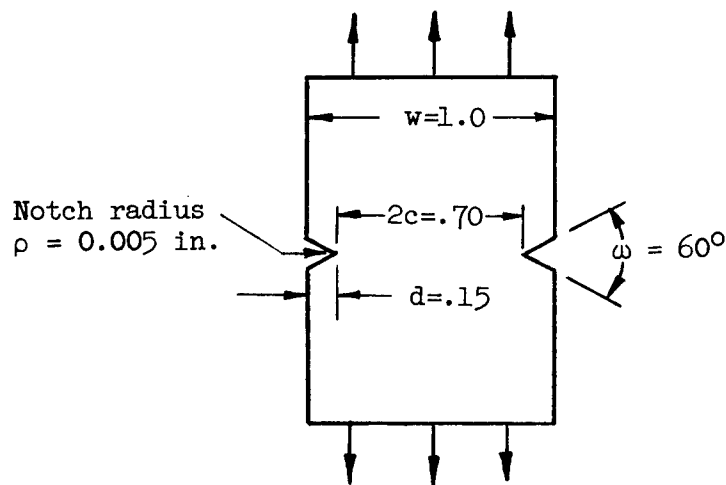
Sketch 1

From equations (8) and (9), respectively,

$$K_S = 1 + 2\sqrt{\frac{0.15}{0.005}} = 11.95$$

and

$$K_D = \frac{4}{\pi}\sqrt{\frac{0.35}{0.005}} = 10.65$$

From equation (10),

$$K_T = 1 + \frac{(10.95)(9.65)}{\sqrt{(10.95)^2 + (9.65)^2}} = 8.23$$

From figure 2,

$$\sqrt{\rho'} = 0.144 \text{ in.}^{1/2}$$

Finally, from equation (1a),

$$K_N = 1 + \frac{7.23}{1 + \dfrac{\pi}{\pi - \dfrac{\pi}{6}} \dfrac{0.144}{\sqrt{0.005}}} = 3.10$$

Static Notch Strength Factors

Symmetrical edge notch.- The static notch strength factor is computed for the specimen shown in sketch 1. The Neuber factor K_N is obtained in the same manner as in the previous example. Thus

$$K_N = 3.10$$

Then from figure 4,

$$K_u = 1.28$$

Finally, the flow-restraint correction is applied according to equation (6):

$$K_u{}^* = \frac{1.28}{1 + 0.096\left(\dfrac{50}{70}\right)\tanh\dfrac{0.005}{0.0208}} = 1.26$$

where $B = 0.096$ is obtained from figure 5.

External crack.- The static notch strength factor is computed for the specimen shown in sketch 2:
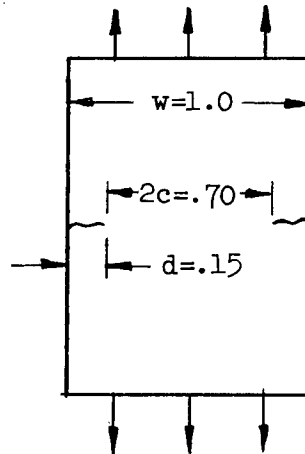
Sketch 2

The factors K_S and K_D are computed from formulas (8) and (9), respectively, with ρ' substituted for ρ; then K_{TN} is computed from formula (10). Thus

$$K_S = 1 + 2 \sqrt{\frac{d}{\rho'}} = 1 + 2 \frac{\sqrt{0.15}}{0.144} = 6.37$$

$$K_D = \frac{4}{\pi} \sqrt{\frac{c}{\rho'}} = \frac{4}{\pi} \frac{\sqrt{0.35}}{0.144} = 5.24$$

and

$$K_T \equiv K_{TN} = 1 + \frac{\left(K_S - 1\right)\left(K_D - 1\right)}{\sqrt{\left(K_S - 1\right)^2 + \left(K_D - 1\right)^2}}$$

$$K_{TN} = 1 + \frac{(5.37)(4.24)}{\sqrt{(5.37)^2 + (4.24)^2}} = 4.33$$

Finally, from figure 4,

$$K_u = K_u{}^* = 1.32$$

$\left(\text{The final static strength factor } K_u{}^* \text{ is equal to } K_u \text{ for a crack since } \tanh \frac{\rho}{\rho'} \approx 0.\right)$

Internal crack.- The static notch strength factor is computed for the specimen shown in sketch 3:
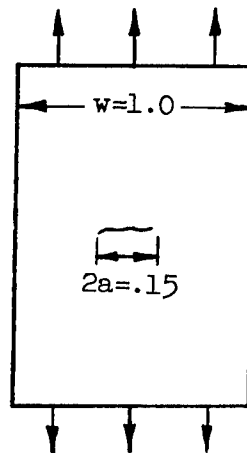
Sketch 3

From equation (12),

$$K_{TN} = 1 + \left(K_C - 1\right) \sqrt{\frac{a}{\rho'}} = 1 + (2.62 - 1)\frac{\sqrt{0.075}}{0.144} = 4.09$$

where $K_C = 2.62$ is obtained from figure 15. Then from figure 4,

$$K_u = K_u{}^* = 1.31$$

REFERENCES

1. Neuber, H.: Theory of Notch Stresses: Principles for Exact Stress Calculation. J. W. Edwards (Ann Arbor, Mich.), 1946. (Kerbspannungslehre: Grundlagen für genaue Spannungsrechnung, Julius Springer (Berlin), 1937.)

2. Kuhn, P.: Effect of Geometric Size on Notch Fatigue. Int. Union of Theor. and Appl. Mech. Colloquium on Fatigue (Stockholm, May 1955), Springer-Verlag (Berlin), 1956, pp. 131-140.

3. Kuhn, Paul, and Hardrath, Herbert F.: An Engineering Method for Estimating Notch-Size Effect in Fatigue Tests on Steel. NACA TN 2805, 1952.

4. McEvily, Arthur J., Jr., Illg, Walter, and Hardrath, Herbert F.: Static Strength of Aluminum-Alloy Specimens Containing Fatigue Cracks. NACA TN 3816, 1956.

5. Committee E-9 on Fatigue, ASTM: Manual on Fatigue Testing. Special Tech. Pub. No. 91, ASTM (Philadelphia), 1949.

6. Peterson, R. E.: Stress Concentration Design Factors. John Wiley & Sons, Inc., c.1953.

7. Stowell, Elbridge Z.: Stress and Strain Concentration at a Circular Hole in an Infinite Plate. NACA TN 2073, 1950.

8. Hardrath, Herbert F., and Ohman, Lachlan: A Study of Elastic and Plastic Stress Concentration Factors Due to Notches and Fillets in Flat Plates. NACA Rep. 1117, 1953. (Supersedes NACA TN 2566.)

9. Templin, R. L.: Fatigue of Aluminum. Proc. ASTM, vol. 54, 1954, pp. 641-699.

10. (a) Anon.: Strength of Metal Aircraft Elements. ANC-5, Munitions Board Aircraft Committee, Dept. of Defense. Revised ed., June 1951.

    (b) Anon.: Strength of Metal Aircraft Elements. MIL-HDBK-5, Armed Forces Supply Support Center, Mar. 1959.

11. Bennett, J. A., and Weinberg, J. G.: Fatigue Notch Sensitivity of Some Aluminum Alloys. Res. Paper 2495, Jour. Res. of Nat. Bur. Standards, vol. 52, no. 5, May 1954, pp. 235-245.

L
1
7
4
3

38

12. Hyler, W. S., Abraham, E. D., and Grover, H. J.: Fatigue Crack Propagation in Severely Notched Bars. NACA TN 3685, 1956.

13. MacGregor, C. W., and Grossman, N.: Effects of Cyclic Loading on Mechanical Behavior of 24S-T4 and 75S-T6 Aluminum Alloys and SAE 4130 Steel. NACA TN 2812, 1952.

14. Mann, J. Y.: The Effect of Stress Concentrations on the Fatigue Resistance of 24ST Aluminium Alloy. Rep. SM.217, Aero. Res. Labs. (Melbourne), Nov. 1953.

15. Moore, H. F.: Aluminum Alloy 75S-T. Part I of The Effect of Size and Notch Sensitivity on Fatigue Characteristics of Two Metallic Materials. Tech. Rep. 5726, Air Materiel Command, U.S. Air Force, Oct. 5, 1948.

16. Hyler, W. S., Lewis, R. A., and Grover, H. J.: Experimental Investigation of Notch-Size Effects on Rotating-Beam Fatigue Behavior of 75S-T6 Aluminum Alloy. NACA TN 3291, 1954.

17. Wallgren, Gunnar: Direct Fatigue Tests With Tensile and Compressive Mean Stresses on 24S-T Aluminium Plain Specimens and Specimens Notched by a Drilled Hole. Rep. No. 48, Aero. Res. Inst. of Sweden (Stockholm), 1953.

18. Brueggeman, W. C., Mayer, M., Jr., and Smith, W. H.: Axial Fatigue Tests at Two Stress Amplitudes of 0.032-Inch 24S-T Sheet Specimens With a Circular Hole. NACA TN 983, 1945.

19. Brueggeman, W. C., Mayer, M., Jr., and Smith, W. H.: Axial Fatigue Tests at Zero Mean Stress of 24S-T Aluminum-Alloy Sheet With and Without a Circular Hole. NACA TN 955, 1944.

20. Brueggeman, W. C., and Mayer, M., Jr.: Axial Fatigue Tests at Zero Mean Stress of 24S-T and 75S-T Aluminum-Alloy Strips With a Central Circular Hole. NACA TN 1611, 1948.

21. Grover, H. J., Hyler, W. S., and Jackson, L. R.: Fatigue Strengths of Aircraft Materials. Axial-Load Fatigue Tests on Edge-Notched Sheet Specimens of 2024-T3 and 7075-T6 Aluminum Alloys and of SAE 4130 Steel With Notch Radii of 0.004 and 0.070 Inch. NASA TN D-111, 1959.

22. Grover, H. J., Bishop, S. M., and Jackson, L. R.: Fatigue Strengths of Aircraft Materials. Axial-Load Fatigue Tests on Notched Sheet Specimens of 24S-T3 and 75S-T6 Aluminum Alloys and of SAE 4130 Steel With Stress-Concentration Factors of 2.0 and 4.0. NACA TN 2389, 1951.

23. Grover, H. J., Bishop, S. M., and Jackson, L. R.: Fatigue Strengths of Aircraft Materials. Axial-Load Fatigue Tests on Notched Sheet Specimens of 24S-T3 and 75S-T6 Aluminum Alloys and of SAE 4130 Steel With Stress-Concentration Factor of 5.0. NACA TN 2390, 1951.

24. Landers, Charles B., and Hardrath, Herbert F.: Results of Axial-Load Fatigue Tests on Electropolished 2024-T3 and 7075-T6 Aluminum-Alloy-Sheet Specimens With Central Holes. NACA TN 3631, 1956.

25. Hartman, Ir A.: Onderzoek Naar de Kerfgevoeligheid van Geplateerd 24 S-T en 75 S-T bij Pulserende Sprongbelasting op Trek. Rep. M.1819, Nationaal Luchtvaartlaboratorium (Amsterdam), 1952.

26. Lazan, B. J., and Blatherwick, A. A.: Fatigue Properties of Aluminum Alloys at Various Direct Stress Ratios. Part I - Rolled Alloys. WADC Tech. Rep. 52-307, Part I, U.S. Air Force, Dec. 1952.

27. Grover, H. J., Hyler, W. S., and Jackson, L. R.: Fatigue Strengths of Aircraft Materials. Axial-Load Fatigue Tests on Notched Sheet Specimens of 24S-T3 and 75S-T6 Aluminum Alloys and of SAE 4130 Steel With Stress-Concentration Factor of 1.5. NACA TN 2639, 1952.

28. Naumann, Eugene C., Hardrath, Herbert F., and Guthrie, David E.: Axial-Load Fatigue Tests of 2024-T3 and 7075-T6 Aluminum-Alloy Sheet Specimens Under Constant- and Variable-Amplitude Loads. NASA TN D-212, 1959.

29. Illg, Walter: Fatigue Tests on Notched and Unnotched Sheet Specimens of 2024-T3 and 7075-T6 Aluminum Alloys and of SAE 4130 Steel With Special Consideration of the Life Range From 2 to 10,000 Cycles. NACA TN 3866, 1956.

30. Finney, J. M., and Mann, J. Y.: Some Flexural Fatigue Tests on 75S-T Aluminium Alloy Sheet Specimens With Drilled Holes. SM Note 213, Aero. Res. Labs. (Melbourne), Nov. 1954.

31. Phillips, C. E., and Fenner, A. J.: Some Fatigue Tests on Aluminum-Alloy and Mild-Steel Sheet, With and Without Drilled Holes. Proc. Inst. Mech. Eng. (London), vol. 165, 1951, pp. 125-129.

32. Taylor, W. J., and Gunn, N. J. F.: The Effect of Notches on the Fatigue Strength of Three Light Alloys. Rep. No. Met.42, British R.A.E., Aug. 1950.

33. Gunn, N. J. F.: Fatigue Properties at Low Temperature on Transverse and Longitudinal Notched Specimens of D.T.D. 363A Aluminium Alloy. Tech. Note No. Met.163, British R.A.E., June 1952.

L
1
7
4
3

40

34. Sorensen, Arne: Some Design Considerations for Tear-Resistant Air-
    plane Structures. Preprint No. 618, S.M.F. Fund Preprint, Inst.
    Aero. Sci., Jan. 1956.

35. Nordmark, Glenn E., and Eaton, Ian D.: Effect of Fatigue Crack on
    Static Strength: 2014-T6, 2024-T4, 6061-T6, 7075-T6 Open-Hole
    Monobloc Specimens. NACA TM 1428, 1957.

36. Hardrath, Herbert F., Landers, Charles B., and Utley, Elmer C., Jr.:
    Axial-Load Fatigue Tests on Notched and Unnotched Sheet Specimens
    of 61S-T6 Aluminum Alloy, Annealed 347 Stainless Steel, and Heat-
    Treated 403 Stainless Steel. NACA TN 3017, 1953.

37. Anon.: Alcoa Aluminum Handbook. Aluminum Co. of America, 1956.

L
1
7
4
3

TABLE I.- EXPERIMENTAL AND COMPUTED FATIGUE FACTORS

(a) 2024-T3 aluminum-alloy specimens, axial load

Gross width, in.	Net width, in.	Thickness, t, in.	Shape of notch	Root radius, ρ, in.	K_T	σ_u, ksi	Fatigue limit (notched), ksi	Fatigue limit (unnotched), ksi	$\sqrt{\rho'}$, in.$^{1/2}$	K_N	K_F	K_N/K_F	Ref.
0.445	0.327	----	Hole	0.058	2.70	76.7	10.0	17.1	0.134	2.01	1.71	1.18	17
.500	.382	0.032	Hole	.0643	2.42	69.9	13.0	22.0	.143	1.90	1.69	1.13	18
.500	.371	.032	Hole	.0643	2.47	72.6	13.0	22.0	.139	1.90	1.69	1.13	19
1.00	.743	.032	Hole	.1285	2.42	72.6	13.0	22.0	.139	2.02	1.69	1.20	19
1.00	.871	.032	Hole	.0643	2.67	72.6	13.0	22.0	.139	2.06	1.69	1.22	19
.25	.23	.032	Hole	.010	2.78	71.5	----	----	.141	1.74	1.30	1.34	20
2.00	1.98	.032	Hole	.010	2.97	71.5	----	----	.141	1.82	1.15	1.58	20
.25	.186	.032	Hole	.032	2.43	71.5	----	----	.141	1.80	1.65	1.09	20
.25	.250	.032	Hole	.063	2.16	71.5	----	----	.141	1.74	1.30	1.34	20
.50	.375	.032	Hole	.063	2.43	71.5	----	----	.141	1.92	1.70	1.13	20
.50	.25	.032	Hole	.125	2.16	71.5	----	----	.141	1.83	1.80	1.02	20
1.00	.75	.032	Hole	.125	2.43	71.5	----	----	.141	2.02	1.85	1.09	20
.50	.124	.032	Hole	.188	2.04	71.5	----	----	.141	1.78	1.80	.99	20
1.00	.50	.032	Hole	.250	2.16	71.5	----	----	.141	1.91	1.65	1.16	20
1.00	.25	.032	Hole	.375	2.04	71.5	----	----	.141	1.85	1.50	1.23	20
2.00	1.00	.032	Hole	.500	2.16	71.5	----	----	.141	1.97	1.70	1.16	20
2.00	.50	.032	Hole	.750	2.04	71.5	----	----	.141	1.90	1.65	1.15	20
.25	.23	.064	Hole	.010	2.78	71.5	----	----	.141	1.74	1.30	1.34	20
.25	.186	.064	Hole	.032	2.43	71.5	----	----	.141	1.80	1.55	1.16	20
.25	.375	.064	Hole	.063	2.16	71.5	----	----	.141	1.74	1.40	1.24	20
.50	.375	.064	Hole	.063	2.43	71.5	----	----	.141	1.92	1.60	1.20	20
.25	.162	.064	Hole	.094	2.04	71.5	----	----	.141	1.72	1.25	1.38	20
1.00	.75	.064	Hole	.125	2.43	71.5	----	----	.141	2.02	1.75	1.16	20
.50	.124	.064	Hole	.188	2.04	71.5	----	----	.141	1.78	1.40	1.27	20
1.00	.50	.064	Hole	.250	2.16	71.5	----	----	.141	1.91	1.70	1.12	20
1.00	.25	.064	Hole	.375	2.04	71.5	----	----	.141	1.85	1.70	1.09	20
4.10	1.50	.090	U	.004	4.00	73.0	10.5	21.0	.138	1.94	2.00	.97	21
1.516	1.498	.090	U	.070	4.00	73.0	7.0	21.0	.138	2.97	3.00	.97	21

TABLE I.- EXPERIMENTAL AND COMPUTED FATIGUE FACTORS - Continued

(a) 2024-T3 aluminum-alloy specimens, axial load - Concluded

Gross width, in.	Net width, in.	Thickness, t, in.	Shape of notch	Root radius, ρ, in.	K_T	σ_w, ksi	Fatigue limit (notched), ksi	Fatigue limit (unnotched), ksi	$\sqrt{\rho'}$, in.$^{1/2}$	K_N	K_F	K_N/K_F	Ref.
4.50	1.50	0.090	Hole	1.500	2.00	73.0	11.0	21.0	0.138	1.90	1.90	1.00	22
2.25	1.50	.090	U	.3175	2.00	73.0	11.5	21.0	.138	1.80	1.82	.99	22
2.25	1.50	.090	U	.057	4.00	73.0	7.5	21.0	.138	2.89	2.80	1.03	22
2.25	1.50	.090	U	.0313	5.00	73.0	6.0	20.5	.138	3.25	3.40	.96	23
4.00	3.875	.090	Hole	.0625	2.91	73.0	9.8	20.5	.138	2.22	2.10	1.06	24
4.00	3.75	.090	Hole	.125	2.82	73.0	8.8	20.5	.138	2.31	2.35	.99	24
4.00	3.50	.090	Hole	.250	2.67	73.0	8.8	20.5	.138	2.31	2.33	.99	24
4.00	3.00	.090	Hole	.500	2.43	73.0	9.4	20.5	.138	2.20	2.19	1.01	24
4.00	2.00	.090	Hole	1.00	2.16	73.0	10.5	20.5	.138	2.02	2.00	1.01	24
2.00	1.938	.090	Hole	.03125	2.91	73.0	10.0	20.5	.138	2.07	2.05	1.01	24
2.00	1.875	.090	Hole	.0625	2.82	73.0	9.5	20.5	.138	2.17	2.16	1.01	24
2.00	1.750	.090	Hole	.125	2.67	73.0	9.4	20.5	.138	2.20	2.18	1.01	24
2.00	1.50	.090	Hole	.250	2.43	73.0	9.8	20.5	.138	2.12	2.10	1.01	24
2.00	1.00	.090	Hole	.500	2.16	73.0	10.0	20.5	.138	1.97	2.05	.96	24
.50	.47	.090	Hole	.015	2.82	73.0	10.0	20.5	.138	1.85	2.05	.90	24
.50	.438	.090	Hole	.031	2.67	73.0	10.0	20.5	.138	1.94	2.05	.94	24
.50	.375	.090	Hole	.0625	2.43	73.0	10.0	20.5	.138	1.92	2.05	.94	24
.50	.250	.090	Hole	.125	2.16	73.0	11.2	20.5	.138	1.83	1.83	1.00	24
1.19	.750	.079	U	.0197	4.79	65.9	5.8	19.0	.150	2.83	3.26	.87	25
.450	.400	----	60° V	.100	1.60	72.8	18.0	21.0	.139	1.39	1.17	1.19	26
.50	.400	----	60° V	.032	2.40	72.8	12.0	21.0	.139	1.72	1.75	.98	26
.450	.400	----	60° V	.010	3.40	72.8	10.0	21.0	.139	1.90	2.10	.91	26
.50	.330	.088	60° V	.0002	27.30	68.0	6.5	20.5	.145	2.95	3.15	.94	(a)
12.00	8.00	.088	60° V	.005	27.30	68.0	2.5	20.5	.145	8.60	8.33	1.03	(a)
3.00	1.50	.090	U	.760	1.50	73.0	16.0	21.0	.138	1.43	1.30	1.10	27
2.25	1.50	.090	U	.058	4.00	72.1	7.5	20.5	.140	2.89	2.73	1.06	28
2.25	1.50	.090	U	.3175	2.00	72.1	11.5	20.0	.140	1.80	1.74	1.03	29
2.25	1.50	.090	U	.057	4.00	72.1	6.5	20.0	.140	2.89	3.08	.94	29

aNASA unpublished data.

TABLE I.- EXPERIMENTAL AND COMPUTED FATIGUE FACTORS - Continued

(b) 2024-T4 aluminum-alloy specimens, rotating beam

Maximum diameter, in.	Minimum diameter, in.	Shape of notch	Root radius, ρ, in.	K_T	σ_u, ksi	Fatigue limit (notched), ksi	Fatigue limit (unnotched), ksi	$\sqrt{\rho'}$, in.$^{1/2}$	K_N	K_F	K_N/K_F	Ref.
0.480	0.330	60° V	0.0002	18.59	68.0	11.0	20.5	0.147	2.30	1.86	1.23	9
.480	.330	60° V	.0002	18.59	62.0	11.0	20.0	.156	2.23	1.82	1.23	10
-----	.300	Fillet	.025	1.79	73.5	16.0	27.5	.138	1.42	1.71	.83	11
-----	.300	Fillet	.0625	1.40	73.5	21.0	27.5	.138	1.26	1.31	.96	11
.312	.250	60° V	.002	5.20	72.4	17.5	25.0	.140	1.88	1.43	1.31	12
.480	.355	U	.0625	1.60	70.5	15.5	20.0	.140	1.38	1.29	1.07	13
.480	.355	45° V	.010	3.10	70.5	9.0	20.0	.143	1.80	2.22	.81	13
.500	.350	45° V	.080	1.50	67.1	17.5	23.0	.148	1.31	1.32	.99	14
.500	.350	45° V	.018	2.50	67.1	11.5	23.0	.148	1.67	2.00	.84	14
.500	.350	45° V	.005	4.30	67.1	9.0	23.0	.148	1.98	2.56	.78	14
.500	.350	45° V	.003	5.50	67.1	8.0	23.0	.148	2.10	2.88	.73	14
.500	.350	45° V	.0005	14.00	67.5	14.5	23.0	.148	2.52	1.59	1.58	14

TABLE I.- EXPERIMENTAL AND COMPUTED FATIGUE FACTORS - Continued

(c) 7075-T6 aluminum-alloy specimens, axial load

Gross width, in.	Net width, in.	Thickness, t, in.	Shape of notch	Root radius, ρ, in.	K_T	σ_u, ksi	Fatigue limit (notched), ksi	Fatigue limit (unnotched), ksi	$\sqrt{\rho'}$, in.$^{1/2}$	K_N	K_F	K_N/K_F	Ref.
0.25	0.186	0.032	Hole	0.032	2.43	83.4	---	---	0.124	1.85	1.95	0.95	20
.25	.125	.032	Hole	.063	2.16	83.4	---	---	.124	1.78	1.90	.94	20
.50	.375	.032	Hole	.063	2.43	83.4	---	---	.124	1.96	2.05	.96	20
.50	.25	.032	Hole	.125	2.16	83.4	---	---	.124	1.86	1.65	1.13	20
1.00	.75	.032	Hole	.125	2.43	83.4	---	---	.124	2.06	2.05	1.00	20
1.00	.50	.032	Hole	.250	2.16	83.4	---	---	.124	1.93	1.90	1.02	20
2.00	1.50	.032	Hole	.250	2.43	83.4	---	---	.124	2.14	1.75	1.22	20
1.00	.25	.032	Hole	.375	2.04	83.4	---	---	.124	1.87	1.80	1.04	20
2.00	1.00	.032	Hole	.500	2.16	83.4	---	---	.124	1.99	1.65	1.21	20
2.00	.50	.032	Hole	.750	2.04	83.4	---	---	.124	1.91	1.60	1.19	20
4.10	1.50	.090	U	.004	4.00	82.5	9.00	21.0	.127	2.00	2.34	.86	21
1.516	1.498	.090	U	.070	4.00	82.5	7.00	21.0	.127	3.03	3.00	1.01	21
2.25	1.50	.090	U	.057	4.00	82.5	7.0	21.0	.127	2.96	3.00	.99	22
4.50	1.50	.090	Hole	1.500	2.00	82.5	11.0	21.0	.127	1.91	1.90	1.01	22
2.25	1.50	.090	U	.3175	2.00	82.5	11.5	21.0	.127	1.82	1.75	1.04	22
2.25	1.50	.090	U	.03125	5.00	82.5	5.6	20.5	.127	3.33	3.68	.91	23
4.00	3.875	.090	Hole	.0625	2.91	82.5	9.5	20.5	.127	2.26	2.16	1.05	24
4.00	3.750	.090	Hole	.125	2.82	82.5	9.0	20.5	.127	2.34	2.28	1.03	24
4.00	2.00	.090	Hole	1.00	2.16	82.5	10.0	20.5	.127	2.04	2.05	1.00	24
2.00	1.938	.090	Hole	.03125	2.91	82.5	10.0	20.5	.127	2.11	2.05	1.03	24
2.00	1.875	.090	Hole	.0625	2.82	82.5	9.5	20.5	.127	2.21	2.16	1.02	24
2.00	1.00	.090	Hole	.500	2.16	82.5	10.8	20.5	.127	1.98	1.90	1.04	24
.50	.47	.090	Hole	.015	2.82	82.5	12.0	20.5	.127	1.89	1.71	1.11	24
.50	.375	.090	Hole	.0625	2.43	82.5	12.0	20.5	.127	1.95	1.71	1.14	24
.50	.250	.090	Hole	.125	2.16	82.5	12.0	20.5	.127	1.85	1.71	1.08	24
1.19	.750	.079	U	.0197	4.79	77.0	6.8	16.9	.135	2.93	2.47	1.19	25
>.450	.400	---	60° V	.100	1.60	82.3	18.0	21.0	.127	1.41	1.17	1.20	26
.450	.400	---	60° V	.010	3.40	82.3	9.5	21.0	.127	1.95	2.21	.88	26
.50	.330	.090	60° V	.0002	27.00	83.4	6.3	20.5	.125	3.27	3.25	1.01	(a)
12.00	8.00	.090	60° V	.005	27.00	83.4	2.2	20.5	.125	9.33	9.32	1.00	(a)
3.00	1.50	.090	U	.760	1.50	82.5	11.5	21.0	.127	1.44	1.82	.79	27
2.25	1.50	.090	U	.058	4.00	83.0	8.0	20.5	.126	2.96	2.57	1.15	28
2.25	1.50	.090	U	.057	4.00	83.0	7.3	18.0	.126	2.96	2.43	1.22	29
2.25	1.50	.090	U	.3175	2.00	83.0	13.5	18.0	.126	1.82	1.33	1.37	29

ᵃNASA unpublished data.

TABLE I.- EXPERIMENTAL AND COMPUTED FATIGUE FACTORS - Continued

(d) 7075-T6 aluminum-alloy specimens, rotating beam and sheet bending

Maximum diameter, in.	Minimum diameter, in.	Shape of notch	Root radius, ρ, in.	K_T	σ_w ksi	Fatigue limit (notched), ksi	Fatigue limit (unnotched), ksi	$\sqrt{\rho'}$, in.$^{1/2}$	K_N	K_F	K_N/K_F	Ref.
0.480	0.330	60° V	0.50	1.09	82.0	22.0	25.0	0.127	1.07	1.13	0.95	9
.480	.330	60° V	.106	1.39	82.0	17.5	25.0	.127	1.27	1.43	.89	9
.480	.330	60° V	.062	1.61	82.0	16.5	25.0	.127	1.37	1.52	.90	9
.480	.330	60° V	.031	2.04	82.0	12.5	25.0	.127	1.56	2.00	.78	9
.480	.330	60° V	.0002	18.59	82.0	9.0	25.0	.127	2.49	2.78	.90	9
.480	.330	60° V	.0002	18.59	86.0	9.0	22.0	.124	2.52	2.44	1.03	10
----	.30	Fillet	.025	1.79	84.5	17.5	23.0	.125	1.41	1.32	1.07	11
----	.30	Fillet	.0625	1.40	84.5	20.5	23.0	.125	1.27	1.12	1.13	11
.480	.355	U	.0625	1.60	83.7	16.0	24.0	.125	1.40	1.50	.93	13
.480	.355	45° V	.010	3.10	83.7	11.5	24.0	.125	1.86	2.08	.89	13
.145	.125	U	.010	2.00	86.2	14.1	32.6	.124	1.45	2.33	.62	14
.29	.25	U	.020	2.00	86.2	17.0	32.0	.124	1.53	1.88	.82	14
.58	.50	U	.040	2.00	86.2	16.4	29.4	.124	1.77	1.79	.99	14
1.16	1.00	U	.080	2.00	86.2	15.1	27.1	.124	1.85	1.79	1.03	14
2.175	1.875	U	.150	2.00	86.2	17.0	25.8	.124	1.94	1.52	1.28	14
.145	.125	U	.010	2.00	87.0	16.0	24.0	.122	1.45	1.50	.97	15
.290	.250	U	.020	2.00	87.0	12.0	25.0	.122	1.53	2.09	.73	15
.580	.500	U	.040	2.00	87.0	11.5	24.0	.122	1.62	2.10	.77	15
1.160	1.000	U	.080	2.00	87.0	15.5	25.0	.122	1.70	1.70	1.00	15
2.030	1.750	U	.140	2.00	87.0	17.0	27.0	.122	1.72	1.59	1.08	15
2.545	1.750	60° V	.001	19.20	87.0	15.0	27.0	.122	4.40	1.80	2.44	15
.625	.315	Hole[b]	.155	1.50	82.5	10.0	17.5	.127	1.38	1.75	.79	30
.625	.389	Hole[b]	.118	1.60	82.5	11.0	17.5	.127	1.44	1.59	.91	30
.625	.465	Hole[b]	.080	1.70	82.5	13.5	17.5	.127	1.48	1.30	1.14	30

[b]Sheet bending tests.

TABLE I.- EXPERIMENTAL AND COMPUTED FATIGUE FACTORS - Continued

(e) Miscellaneous aluminum-alloy specimens, axial load

Material	Gross width, in.	Net width, in.	Thickness, t, in.	Shape of notch	Root radius, ρ, in.	K_T	σ_w, ksi	Fatigue limit (notched), ksi	Fatigue limit (unnotched), ksi	$\sqrt{\rho'}$, in.$^{1/2}$	K_N	K_F	K_N/K_F	Ref.
D.T.D.646B	4.57	4.50	0.080	Hole	0.0375	2.70	73.9	----	---	0.138	1.99	1.40	[c]1.05	31
D.T.D.646B	4.53	4.50	.080	Hole	.0156	3.00	73.9	----	---	.138	1.95	1.03	[c]1.40	31
D.T.D.646B	4.625	4.50	.080	Hole	.0625	2.92	73.9	----	---	.138	2.24	1.21	[c]1.37	31
D.T.D.646B	5.00	4.50	.080	Hole	.250	2.70	73.9	----	---	.138	2.33	1.29	[c]1.34	31
D.T.D.646B	6.00	4.50	.080	Hole	.750	2.32	73.9	----	---	.138	2.14	1.50	[c]1.06	31
D.T.D.646B	9.06	9.0	.080	Hole	.0313	3.00	73.9	----	---	.138	2.12	1.20	[c]1.31	31
D.T.D.646B	9.50	9.0	.080	Hole	.125	2.92	73.9	----	---	.138	2.38	1.36	[c]1.30	31
D.T.D.646B	10.0	9.0	.080	Hole	.50	2.70	73.9	----	---	.138	2.42	1.22	[c]1.47	31
D.T.D.646B	12	9.0	.080	Hole	1.50	2.32	73.9	----	---	.138	2.17	1.22	[c]1.32	31
2014-T6	.450	.400	-----	U	.100	1.60	71.6	21.0	24.0	.141	1.41	1.14	1.23	26
2014-T6	.500	.400	-----	U	.032	2.40	71.6	13.5	24.0	.141	1.78	1.78	1.00	26
2014-T6	.450	.400	-----	U	.010	3.40	71.6	9.5	24.0	.141	2.00	2.53	.79	26

[c] $K_N/1.35 K_F$ as noted in reference 31.

47

TABLE I.- EXPERIMENTAL AND COMPUTED FATIGUE FACTORS - Concluded

(f) Miscellaneous aluminum-alloy specimens, rotating beam

Material	Maximum diameter, in.	Minimum diameter, in.	Shape of notch	Root radius, ρ, in.	K_T	σ_w ksi	Fatigue limit (notched), ksi	Fatigue limit (unnotched), ksi	$\sqrt{\rho'}$, in.$^{1/2}$	K_N	K_F	K_N/K_F	Ref.
2025-T6	0.480	0.330	60° V	0.062	1.61	58.0	11.5	16.0	0.127	1.34	1.40	0.96	9
2025-T6	.480	.330	60° V	.031	1.98	58.0	10.0	16.0	.127	1.46	1.60	.92	9
2025-T6	.480	.330	60° V	.0002	18.59	58.0	7.5	16.0	.127	2.18	2.13	1.02	9
2014-T6	.480	.330	60° V	.0002	18.59	67.0	9.0	18.0	.147	2.30	2.00	1.15	10
6061-T6	.480	.330	60° V	.0002	18.59	42.0	7.0	14.0	.209	1.94	2.00	.97	10
6061-T6	-----	.30	Fillet	.025	1.79	48.0	14.5	25.0	.190	1.36	1.73	.79	11
6061-T6	-----	.30	Fillet	.0625	1.40	48.0	21.0	25.0	.190	1.23	1.19	1.03	11
B.S.S.6L1	.40	.32	30.5° V	.01	2.93	75.0	9.4	23.5	.136	1.78	2.50	.71	32
B.S.S.6L1	.40	.32	45° V	.01	2.93	75.0	11.1	23.5	.136	1.76	2.10	.84	32
B.S.S.6L1	.40	.32	60° V	.01	2.93	75.0	11.4	23.5	.136	1.73	2.06	.84	32
B.S.S.6L1	.40	.32	75° V	.01	2.93	75.0	11.0	23.5	.136	1.58	2.15	.73	32
B.S.S.6L1	.40	.28	60° V	.01	2.85	75.0	10.3	23.5	.136	1.70	2.29	.74	32
B.S.S.6L1	.40	.24	60° V	.01	2.75	75.0	9.0	23.5	.136	1.67	2.63	.63	32
B.S.S.6L1	.40	.32	60° V	.02	2.33	75.0	11.6	23.5	.136	1.62	2.02	.80	32
B.S.S.6L1	.40	.32	62° V	.04	1.75	75.0	15.7	23.5	.136	1.40	1.50	.93	32
B.S.S.6L1	.40	.32	U	.04	1.74	75.0	14.3	23.5	.136	1.28	1.64	.78	32
B.S.S.6L1	.40	.32	20° V	.01	2.93	75.0	12.1	23.5	.136	1.79	1.95	.92	32
B.S.S.6L1	.40	.36	60° V	.01	2.83	75.0	12.3	23.5	.136	1.70	1.91	.89	32
B.S.S.6L1	.40	.32	100° V	.01	2.93	75.0	11.9	23.5	.136	1.56	1.99	.78	32
B.S.S.6L1	.40	.20	60° V	.01	2.59	75.0	7.6	23.5	.136	1.60	3.09	.52	32
D.T.D.683	.40	.32	30.5° V	.01	2.93	81.8	11.0	18.7	.127	1.82	1.70	1.07	32
D.T.D.683	.40	.32	45° V	.01	2.93	81.8	10.6	18.7	.127	1.79	1.77	1.01	32
D.T.D.683	.40	.32	60° V	.01	2.93	81.8	9.3	18.7	.127	1.77	2.02	.88	32
D.T.D.683	.40	.32	75° V	.01	2.93	81.8	9.9	18.7	.127	1.89	1.89	1.00	32
D.T.D.683	.40	.28	60° V	.01	2.85	81.8	9.9	18.7	.127	1.73	1.89	.92	32
D.T.D.683	.40	.24	V	.01	2.75	81.8	11.0	18.7	.127	1.69	1.70	.99	32
D.T.D.683	.40	.32	62° V	.02	2.33	81.8	11.0	18.7	.127	1.62	1.70	.95	32
D.T.D.683	.40	.32	U	.04	1.75	81.8	13.5	18.7	.127	1.40	1.39	1.01	32
D.T.D.683	.40	.32	20° V	.04	1.74	81.8	17.7	18.7	.127	1.44	1.06	1.36	32
D.T.D.683	.40	.32	20° V	.01	2.93	81.8	9.5	18.7	.127	1.82	1.97	.92	32
D.T.D.683	.40	.36	60° V	.01	2.83	81.8	9.9	18.7	.127	1.73	1.89	.92	32
D.T.D.683	.40	.32	100° V	.01	2.93	81.8	11.0	18.7	.127	1.59	1.70	.94	32
D.T.D.683	.40	.20	60° V	.01	2.59	81.8	7.7	18.7	.127	1.63	2.43	.67	32
D.T.D.363A	.40	.32	60° V	.01	2.93	86.2	13.8	25.0	.123	1.78	1.81	.98	33

TABLE II.- SUMMARY OF TABLES I(a) TO I(d)

AND FIGURES 10(a) TO 10(d)

Material	Type of loading	Total no. of test points	Av. K_N/K_F	% of points between ±10%	% of points between ±20%
7075-T6	Axial	34	1.05	59	85
7075-T6	Rotating beam and sheet bending	24	1.00	50	71
2024-T3	Axial	56	1.09	59	84
2024-T4	Rotating beam	12	1.03	25	50

L
1
7
4
3

TABLE III.- EXPERIMENTAL AND COMPUTED STATIC NOTCH FACTORS

(a) Specimens with circular holes

| Material	Gross width, in.	Hole radius, ρ, in.	K_T	K_N	Calc. $K_u{}^*$	Exp. K_u	$K_u{}^*/K_u$	Ref.
2024-T3	4.0	0.062	2.91	2.23	1.08	1.16	0.93	24
	4.0	.125	2.82	2.31	1.09	1.14	.95	24
	4.0	.250	2.67	2.31	1.09	1.14	.95	24
	4.0	.500	2.43	2.20	1.08	1.08	1.00	24
	4.0	1.00	2.16	2.02	1.07	1.03	1.04	24
	2.0	.032	2.91	2.08	1.07	1.12	.96	24
	2.0	.062	2.82	2.17	1.07	1.16	.92	24
	2.0	.125	2.67	2.20	1.08	1.14	.95	24
	2.0	.250	2.43	2.12	1.07	1.10	.97	24
	2.0	.500	2.16	1.97	1.07	1.08	.99	24
	.5	.016	2.82	1.85	1.09	1.09	1.00	24
	.5	.032	2.67	1.94	1.05	1.07	.98	24
	.5	.062	2.43	1.92	1.05	1.04	1.01	24
	.5	.125	2.16	1.84	1.05	1.06	.99	24
	35.0	.50	2.92	2.61	1.10	1.24	.89	4
	12.0	.50	2.77	2.48	1.09	1.119	.92	4
	1.0	.094	2.54	2.06	1.06	1.08	.98	(a)
2024-T4	7.5	.25	2.81	2.39	1.13	1.13	1.00	36
7075-T6	4.0	.062	2.91	2.26	.98	1.04	.94	24
	4.0	.125	2.82	2.34	.99	1.03	.96	24
	4.0	1.00	2.16	2.04	.97	1.00	.97	24
	4.0	.032	2.91	2.11	.97	1.00	.97	24
	2.0	.062	2.82	2.21	.98	1.04	.94	24
	2.0	.500	2.16	1.98	.97	.96	1.01	24
	.5	.016	2.16	1.89	.99	.96	1.03	24
	.5	.062	2.43	1.95	.96	.94	1.02	24
	.5	.125	2.16	1.85	.96	1.00	.96	24
	35.0	.50	2.92	2.63	1.01	1.01	1.00	4
	12.0	.50	2.77	2.50	.99	1.03	.96	4
	7.50	.25	2.81	2.46	.96	1.00	.96	36
2014-T6	7.50	.25	2.81	2.40	.95	1.03	.92	36
6061-T6	7.50	.25	2.81	2.29	.89	.99	.90	36

[a]NASA unpublished data.

TABLE III.- EXPERIMENTAL AND COMPUTED STATIC NOTCH FACTORS - Continued

(b) Specimens with internal notches

Material	Gross width, in.	Notch length, in.	Root radius, ρ, in.	K_T	K_N	Calc. $K_u{}^*$	Exp. K_u	$K_u{}^*/K_u$	Ref.
2024-T3	12.0	2.46	[b]0.002	38.3	10.02	1.46	1.50	0.97	4
2024-T4	7.50	1.51	[c].125	4.72	3.86	1.20	1.31	.92	36
2014-T6	7.50	1.51	[c].125	4.72	3.88	1.05	1.10	.95	36
6061-T6	7.50	1.69	[c].125	4.82	3.72	.96	.99	.97	36
7075-T6	7.50	1.34	[c].125	4.61	3.90	1.15	1.14	1.01	36

[b]Thread cut.
[c]Stop drilled at end of crack.

TABLE III.- EXPERIMENTAL AND COMPUTED STATIC NOTCH FACTORS - Continued

(c) Specimens with U-notches

Material	Gross width, in.	Notch depth, in.	Hole radius, ρ, in.	K_T	K_N	Calc. K_u^*	Exp. K_u	K_u^*/K_u	Ref.
2024-T3	12.0	1.75	0.875	2.57	2.37	1.08	1.04	1.08	4
	2.25	.375	.375	1.88	1.72	1.06	.98	.98	4
	12.0	2.0	.005	27.3	9.83	1.40	1.48	.95	4
	12.0	2.0	.005	27.3	9.83	1.40	1.43	.98	(a)
	2.25	.375	.760	1.50	1.43	1.06	.96	1.10	27
	2.25	.375	.3175	2.00	1.80	1.06	.98	1.08	23
	2.25	.375	.057	4.00	2.89	1.13	1.11	1.02	23
	2.25	.375	.03125	5.00	3.25	1.17	1.17	1.00	23
	1.516	.0093	.0035	4.00	1.90	1.17	1.19	.99	23
	4.10	1.30	.071	4.00	2.86	1.13	1.05	1.07	23
7075-T6	12.0	1.75	.875	2.57	2.38	.98	.97	1.01	4
	2.25	.375	.375	1.88	1.73	.96	.92	1.04	4
	12.0	1.75	.005	27.3	10.26	2.00	2.08	.96	4
	12.0	1.75	.005	27.3	10.26	2.00	2.25	.89	4
	2.25	.375	.760	1.50	1.44	.98	.95	1.03	27
	2.25	.375	.3175	2.00	1.82	.96	.94	1.02	23
	2.25	.375	.057	4.00	2.96	1.05	1.00	1.05	23
	2.25	.375	.03125	5.00	3.33	1.11	1.06	1.05	23
	1.516	.0093	.0035	4.00	1.95	1.08	1.08	1.00	23
	4.10	1.30	.071	4.00	3.03	1.05	1.03	1.02	23
6061-T6	2.25	.375	.3175	2.00	1.74	.89	.94	.95	36
	2.25	.375	.3175	2.00	1.74	.89	.96	.93	36
	2.25	.375	.3175	2.00	1.74	.89	.96	.93	36
	2.25	.375	.057	4.00	2.61	.93	.94	.99	36
	2.25	.375	.057	4.00	2.61	.93	.95	.98	36

[a]NASA unpublished data.

L
1
7
4
3

TABLE III.- EXPERIMENTAL AND COMPUTED STATIC NOTCH FACTORS - Concluded

(d) Specimens with 60° V-notches

Material	Gross width, in.	Notch depth, in.	Root radius, ρ, in.	K_T	K_N	Calc. $K_u{}^*$	Exp. K_u	$K_u{}^*/K_u$	Ref.
2024-T3	12.0	2.0	0.005	27.3	8.80	1.36	1.46	0.93	4
	12.0	2.0	.005	27.3	8.80	1.36	1.43	.95	(a)
	12.0	2.0	.005	27.3	8.80	1.36	1.42	.96	(a)
↓	12.0	2.0	.005	27.3	8.80	1.36	1.45	.94	(a)
7075-T6	12.0	2.0	.005	27.3	9.22	1.89	2.15	.88	4
	12.0	2.0	.005	27.3	9.22	1.89	1.90	1.00	(a)
	12.0	2.0	.005	27.3	9.22	1.89	2.02	.93	(a)
↓	12.0	2.0	.005	27.3	9.22	1.89	2.14	.88	(a)

[a]NASA unpublished data.

L-1743
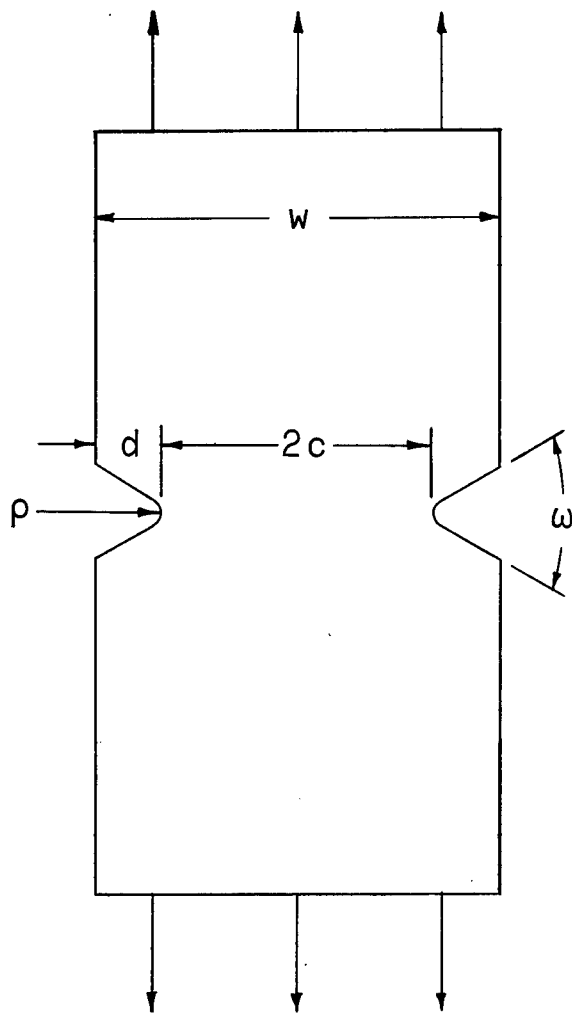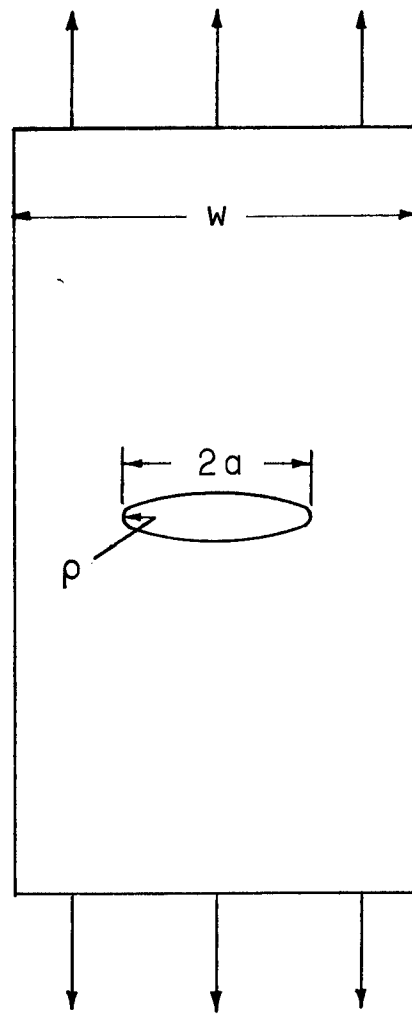
(a) External notch.

(b) Internal notch.

Figure 1.- Notch configurations.
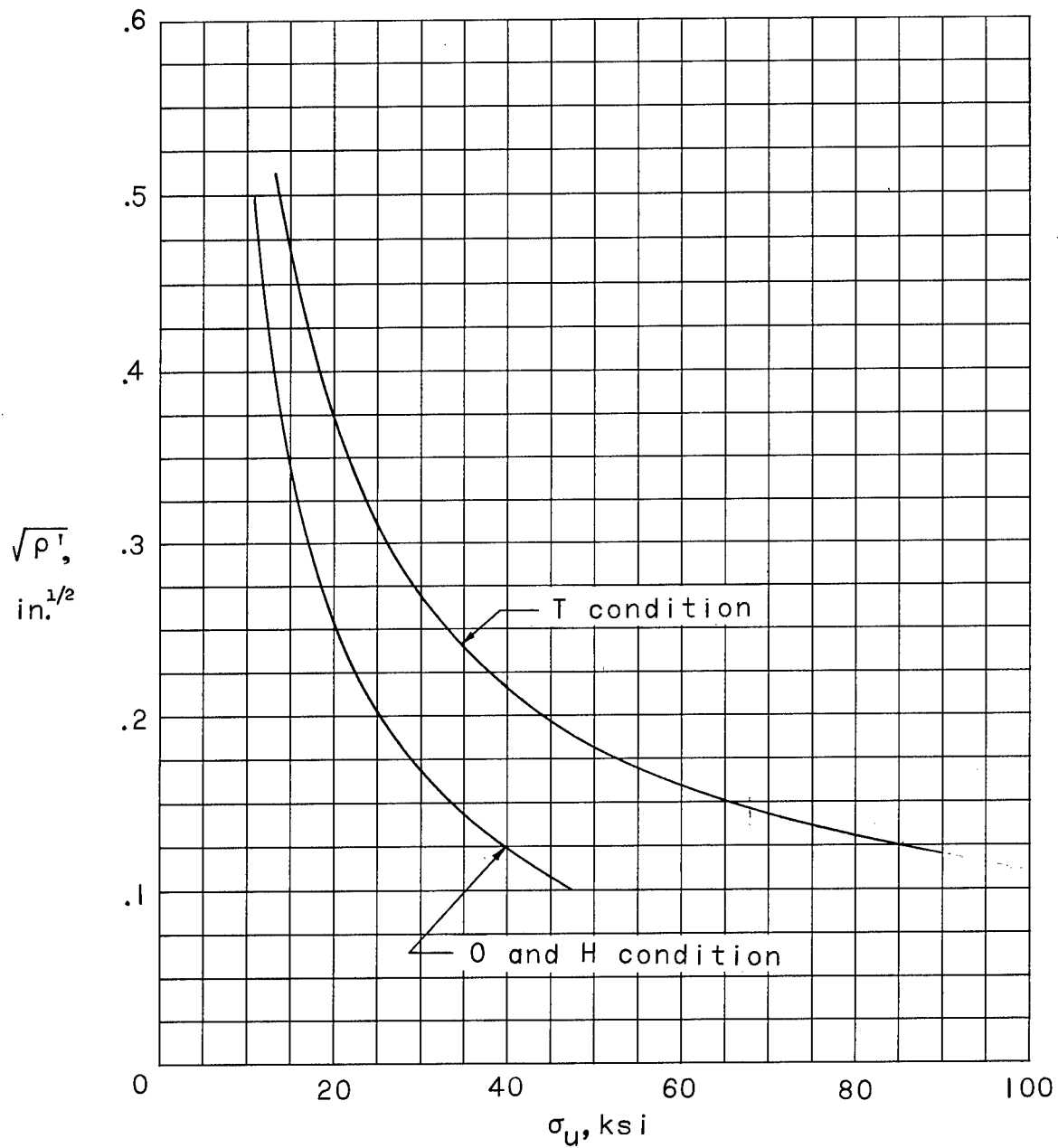
Figure 2.- Neuber constants for wrought aluminum alloys.

L-1743
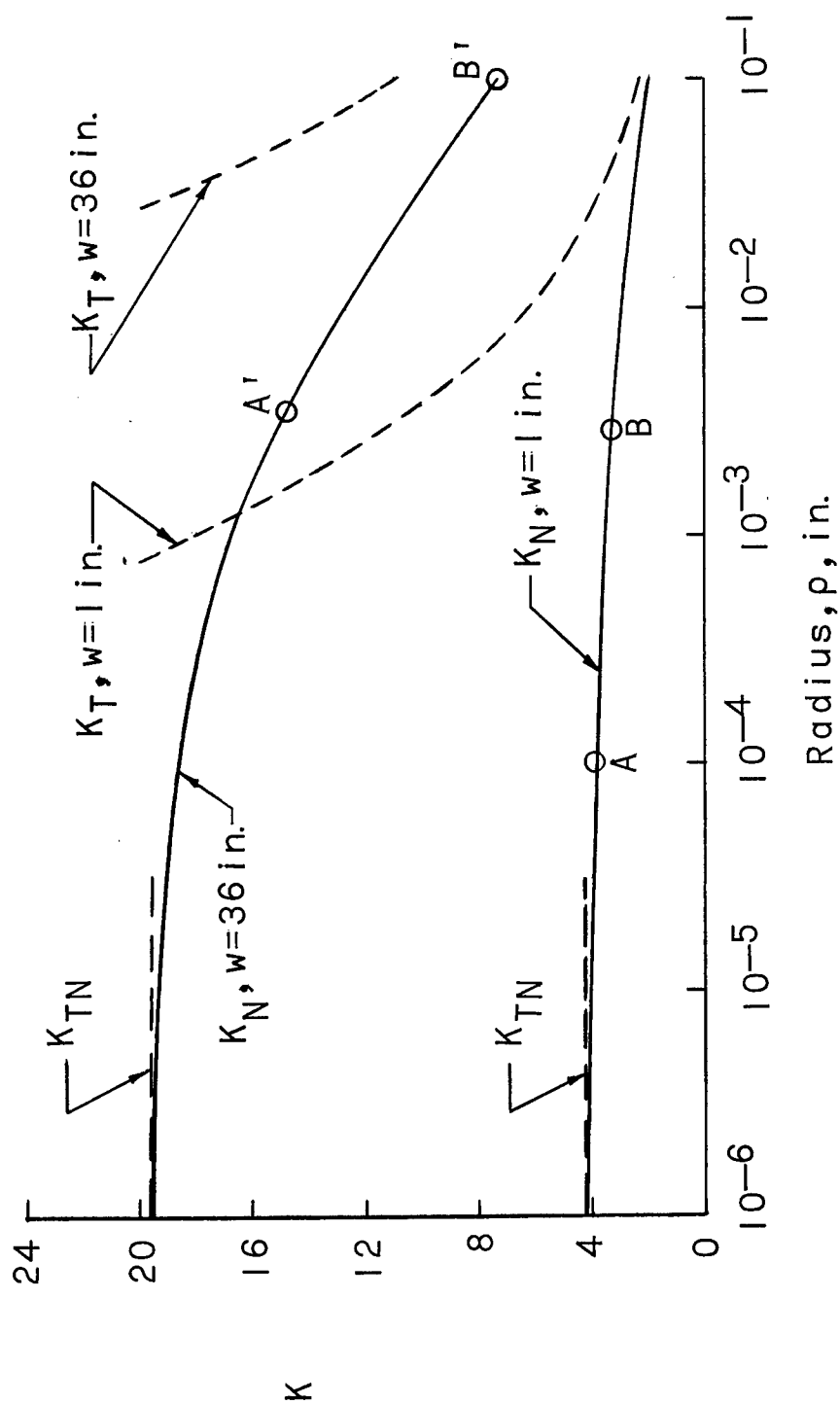
Figure 3.- Variation in stress-concentration factors for heat-treated aluminum alloy with $\sigma_u = 68$ ksi.
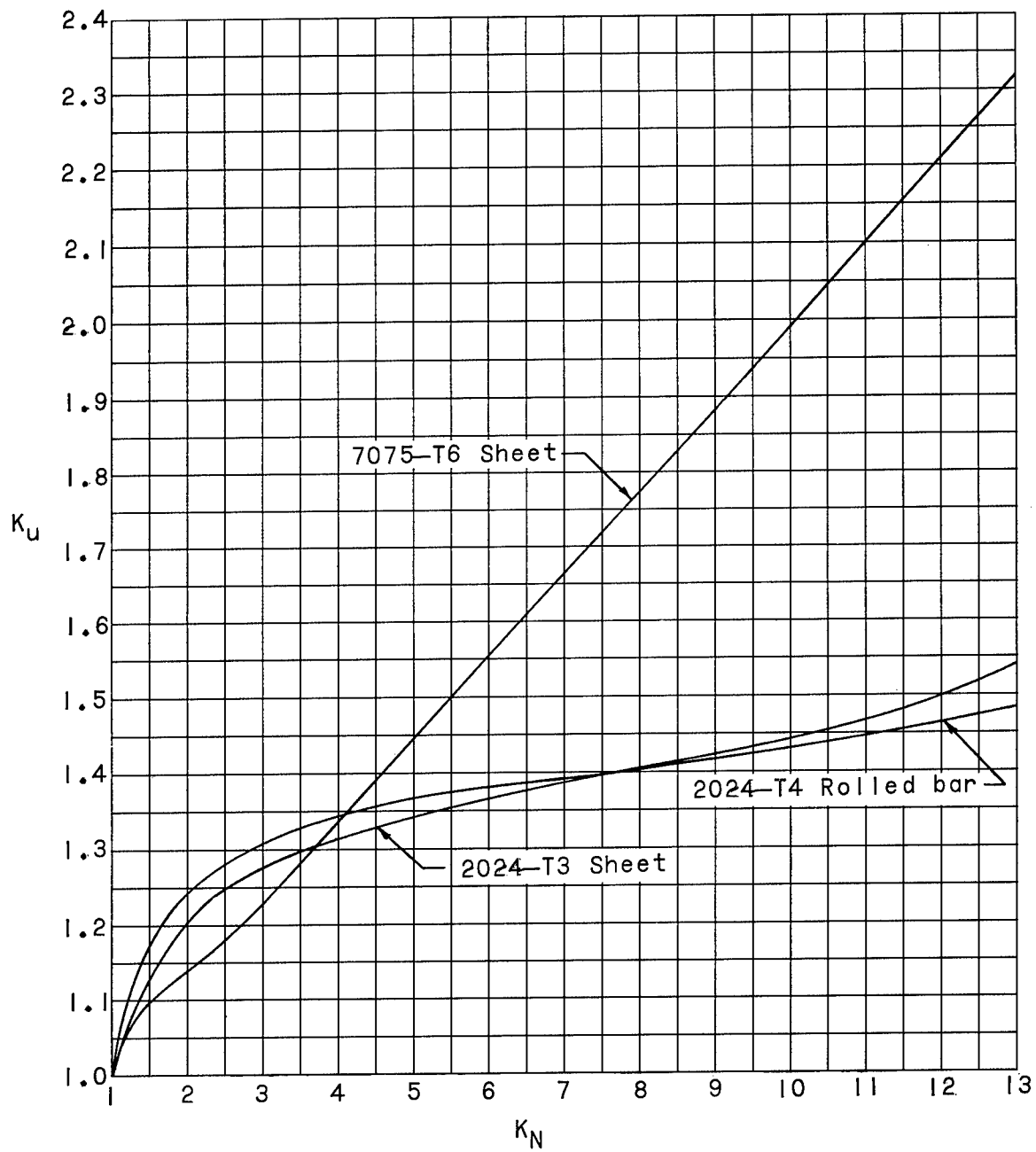
Figure 4.- Typical relations between K_u and K_N.

L-1743

For $K_T > 5$

$$B = .25 \left[1 - \tanh 0.1 (K_T - 1) \right]$$
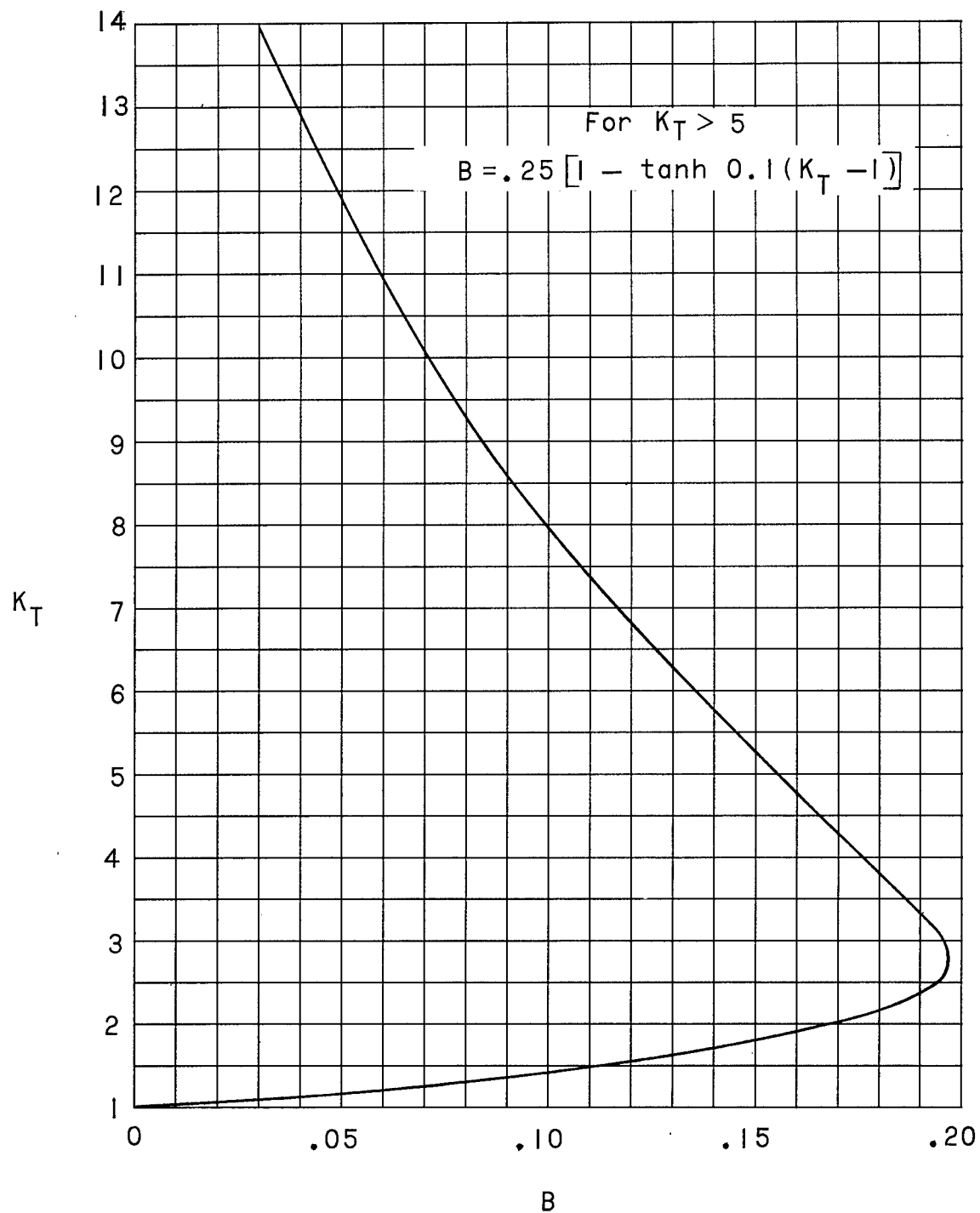
Figure 5.- Flow-restraint factor B.
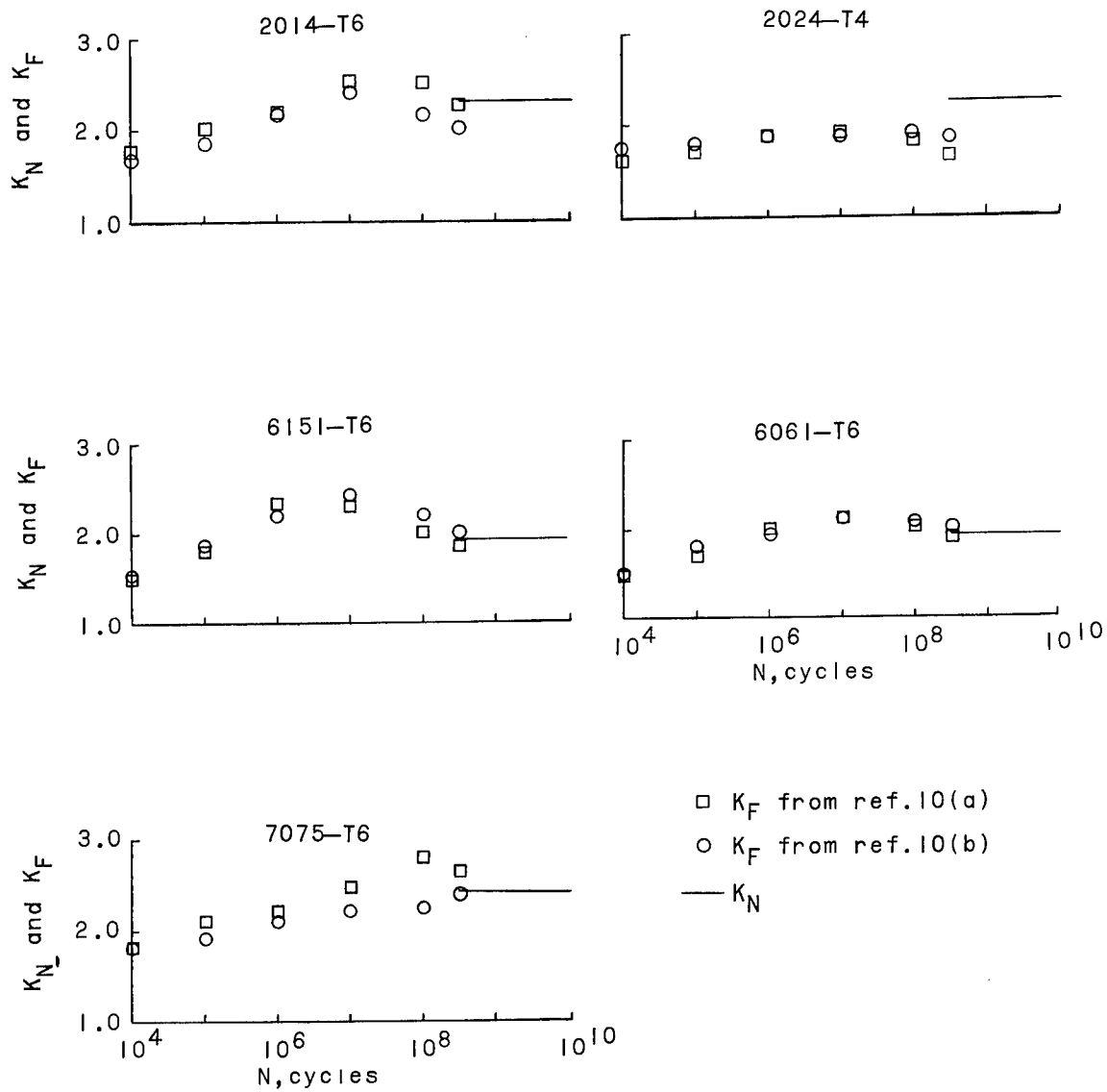
Figure 6.- Experimental fatigue factors K_F and predicted fatigue factors K_N as functions of number of cycles for rotating beams.
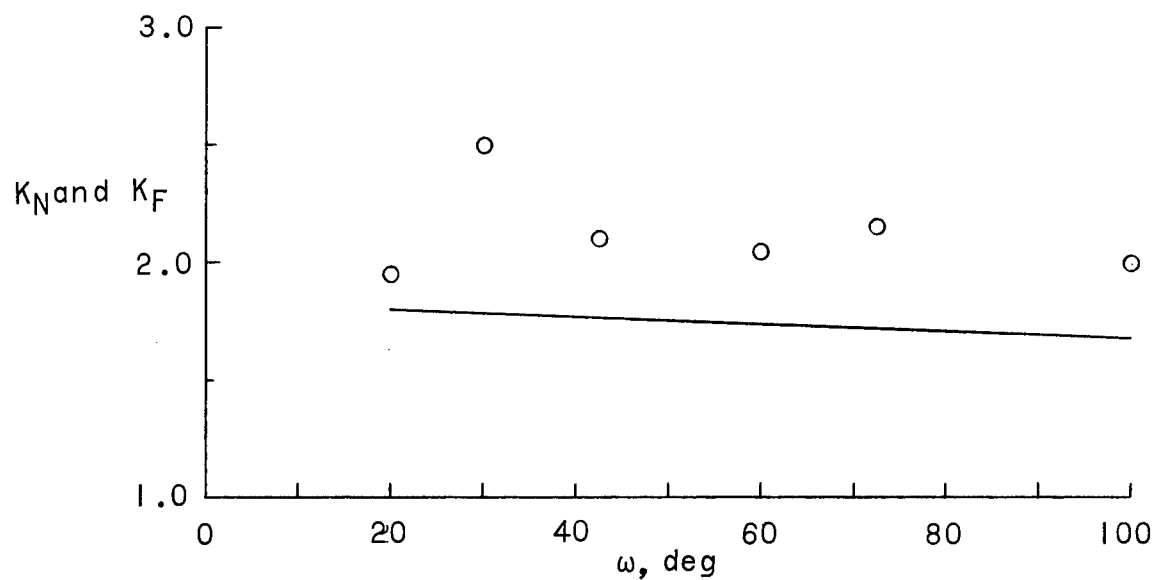
(a) B.S.S.6L1.
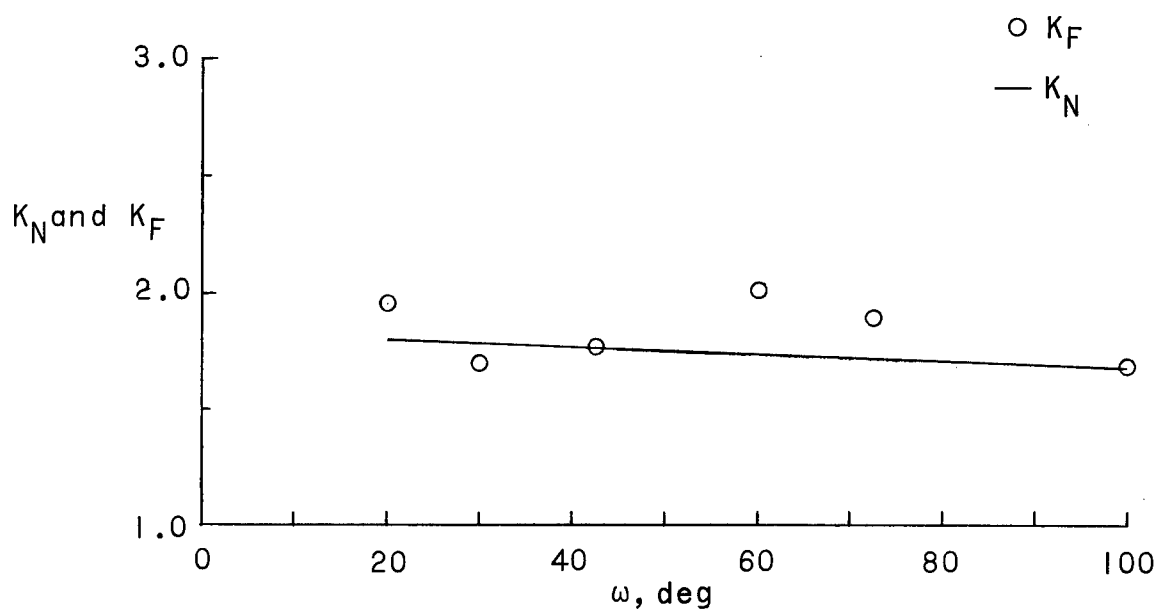
(b) D.T.D.683.

Figure 7.- Experimental fatigue factors K_F and predicted fatigue factors K_N as functions of flank angle. (Data from ref. 32.)
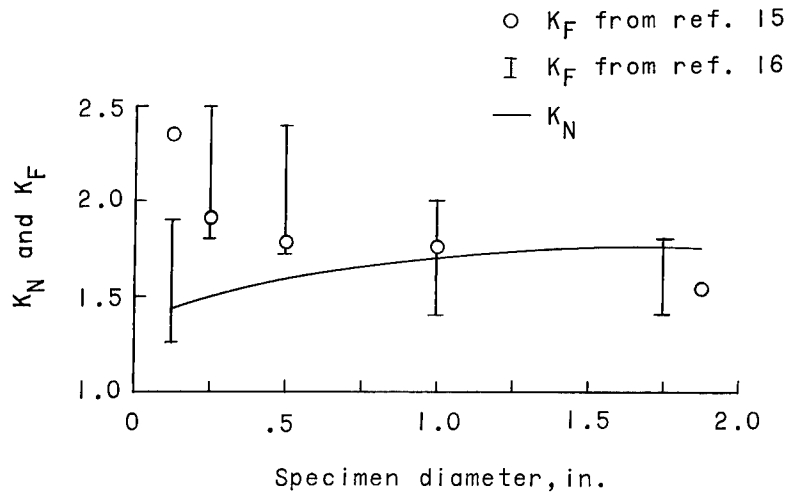
(a)
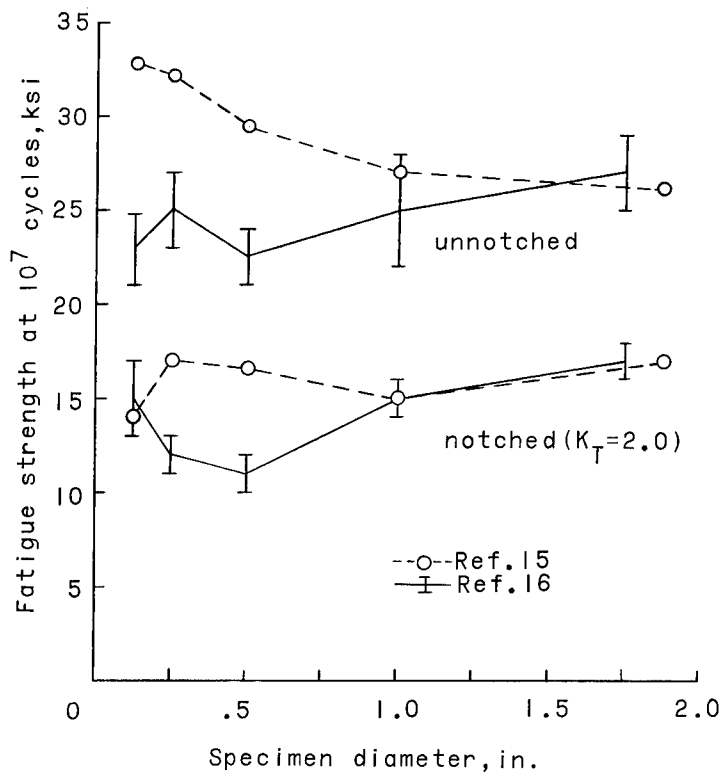
(b)

Figure 8.- Comparison of rotating-beam fatigue results for 7075-T6 obtained at two laboratories.

L-1743
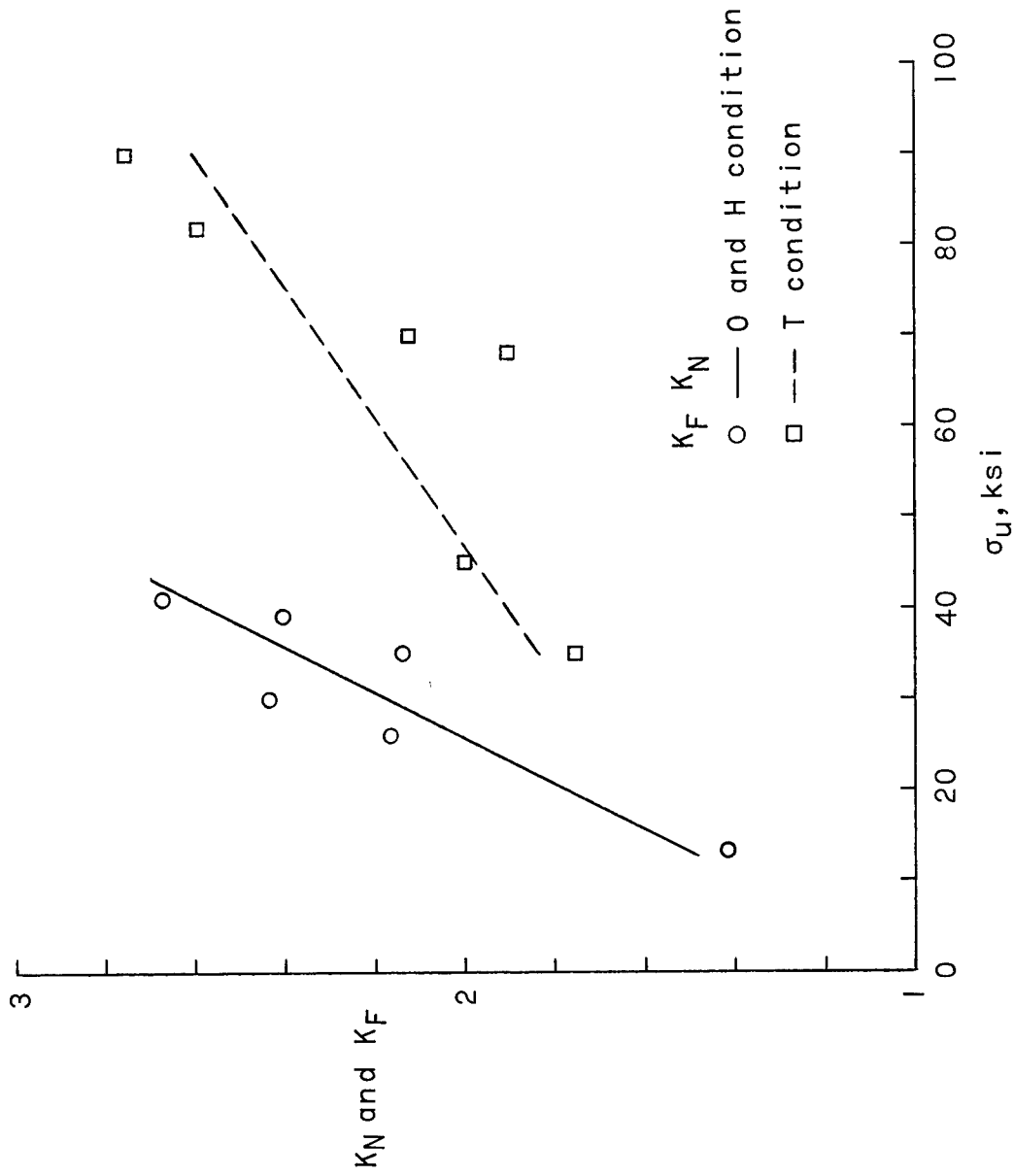
Figure 9.- Experimental fatigue factors K_F and predicted fatigue factors K_N for base data from reference 9.
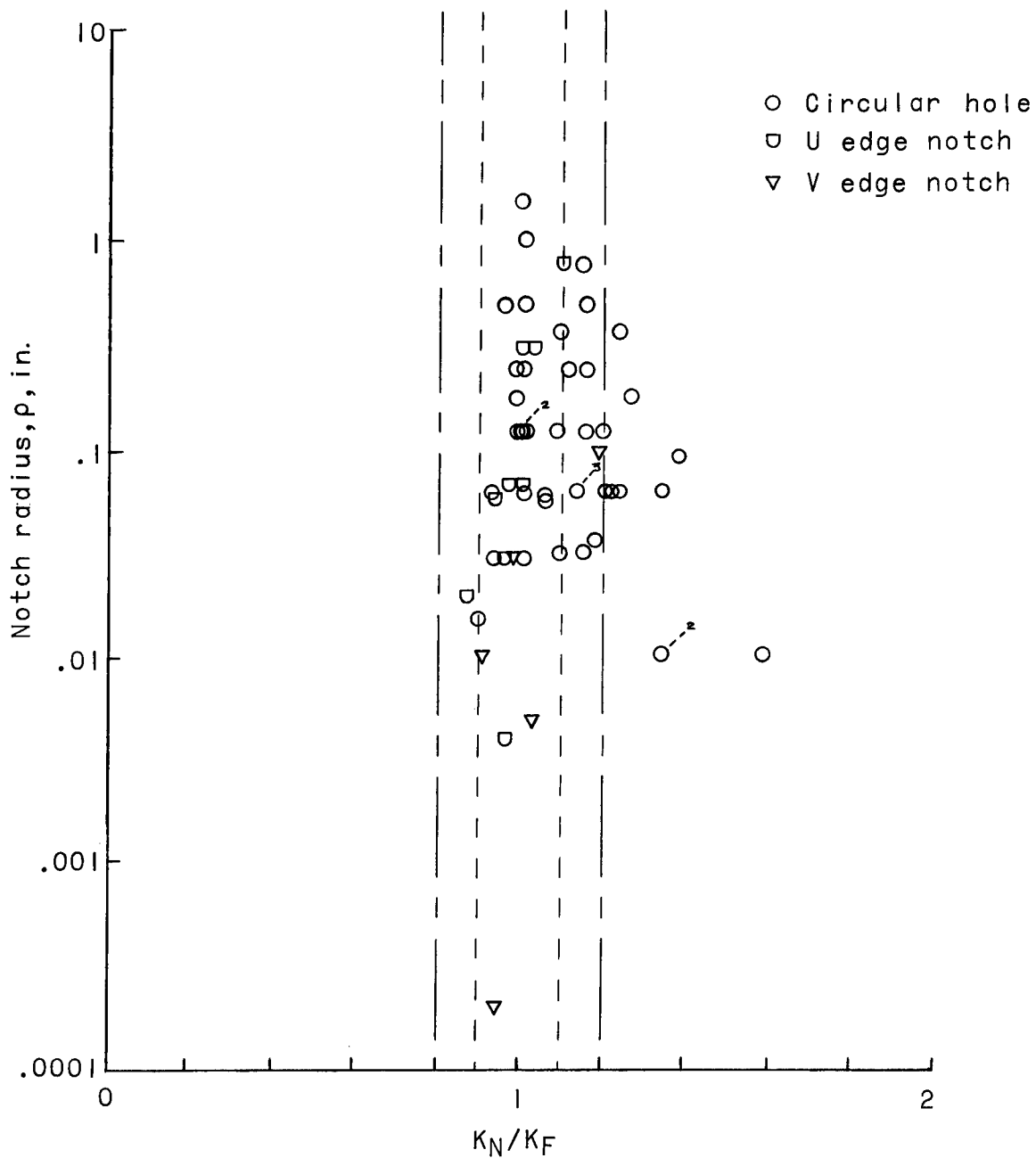
(a) 2024-T3 aluminum-alloy specimens, axial load.

Figure 10.- Ratio of predicted to experimental fatigue factors as a function of notch radius.
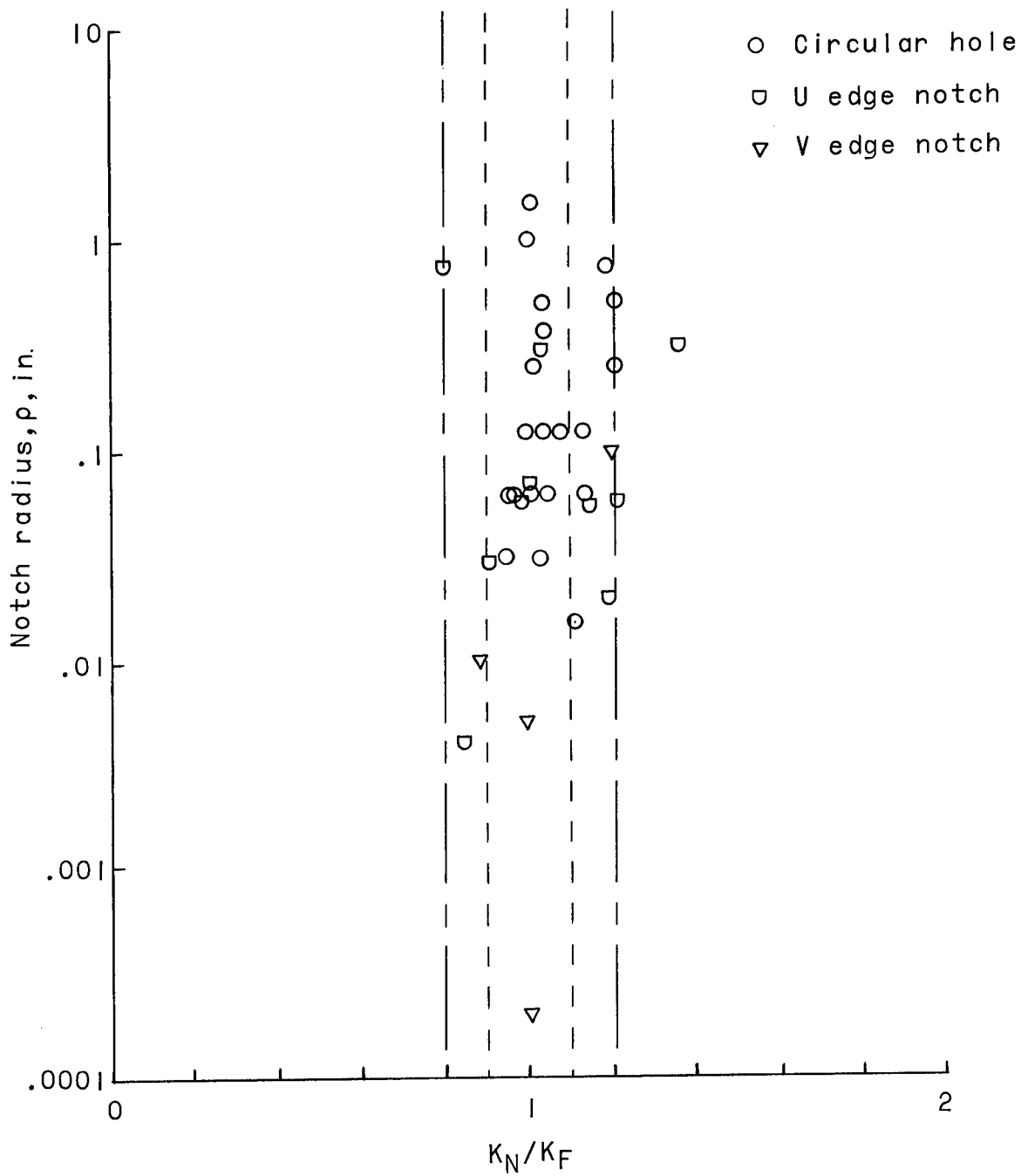
L-1743

Notch radius, ρ, in.

K_N/K_F

□ U edge notch
▽ V edge notch
◁ Fillet

(b) 2024-T4 aluminum-alloy specimens, rotating beam.

Figure 10.- Continued.

(c) 7075-T6 aluminum-alloy specimens, axial load.

Figure 10.- Continued.

L-1743
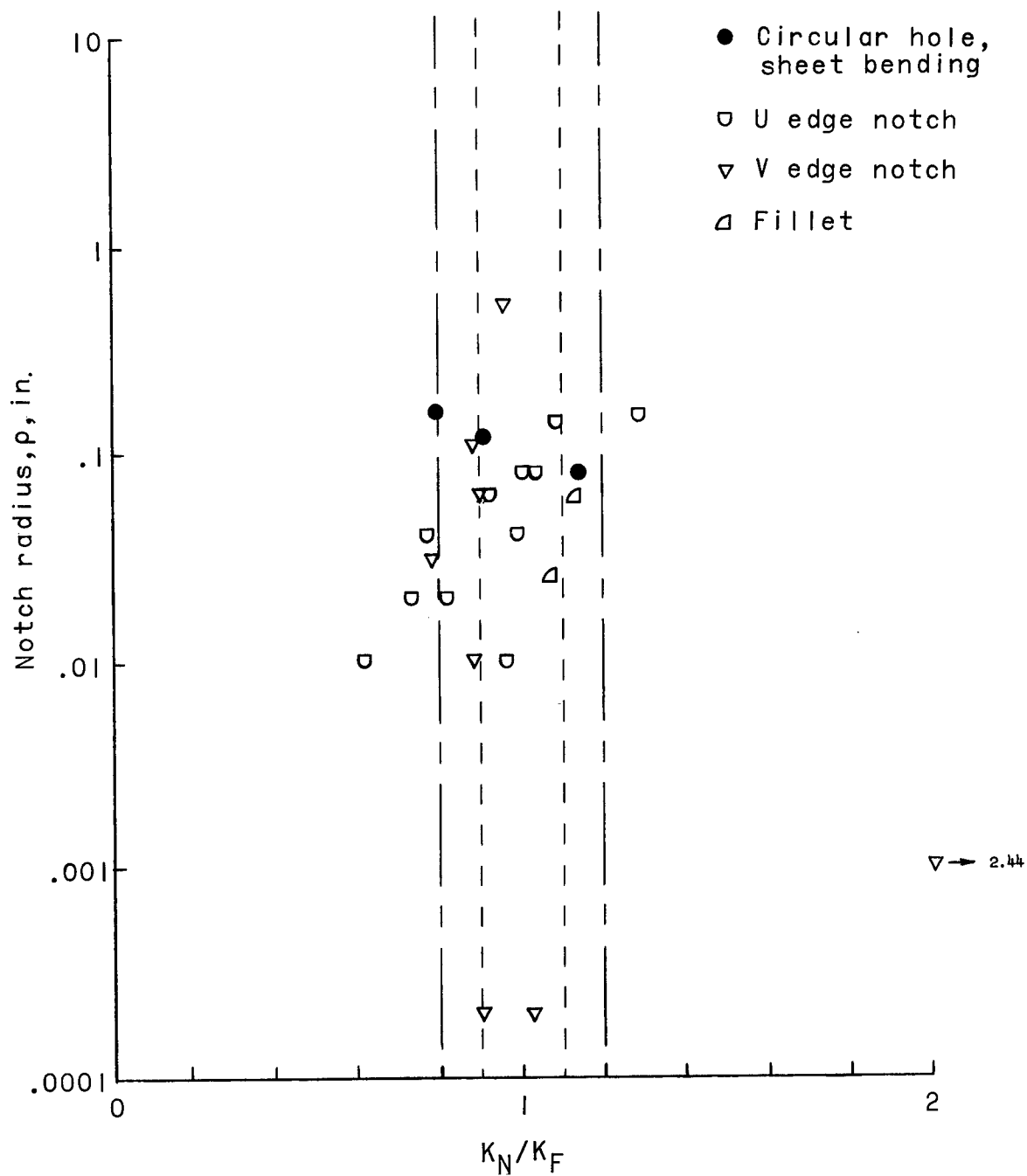
(d) 7075-T6 aluminum-alloy specimens, rotating beam and sheet bending.

Figure 10.- Continued.
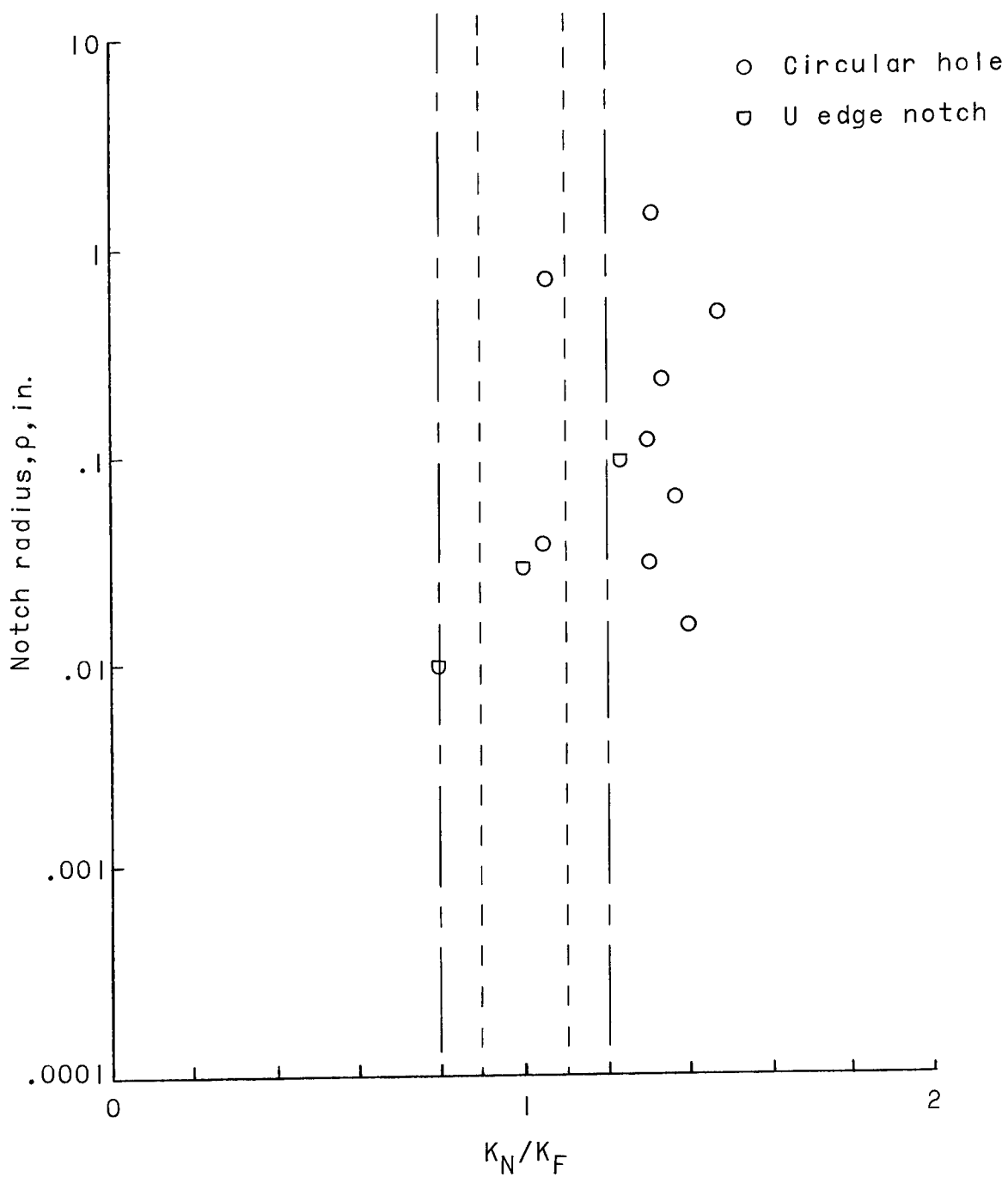
(e) Miscellaneous aluminum-alloy specimens, axial load.

Figure 10.- Continued.
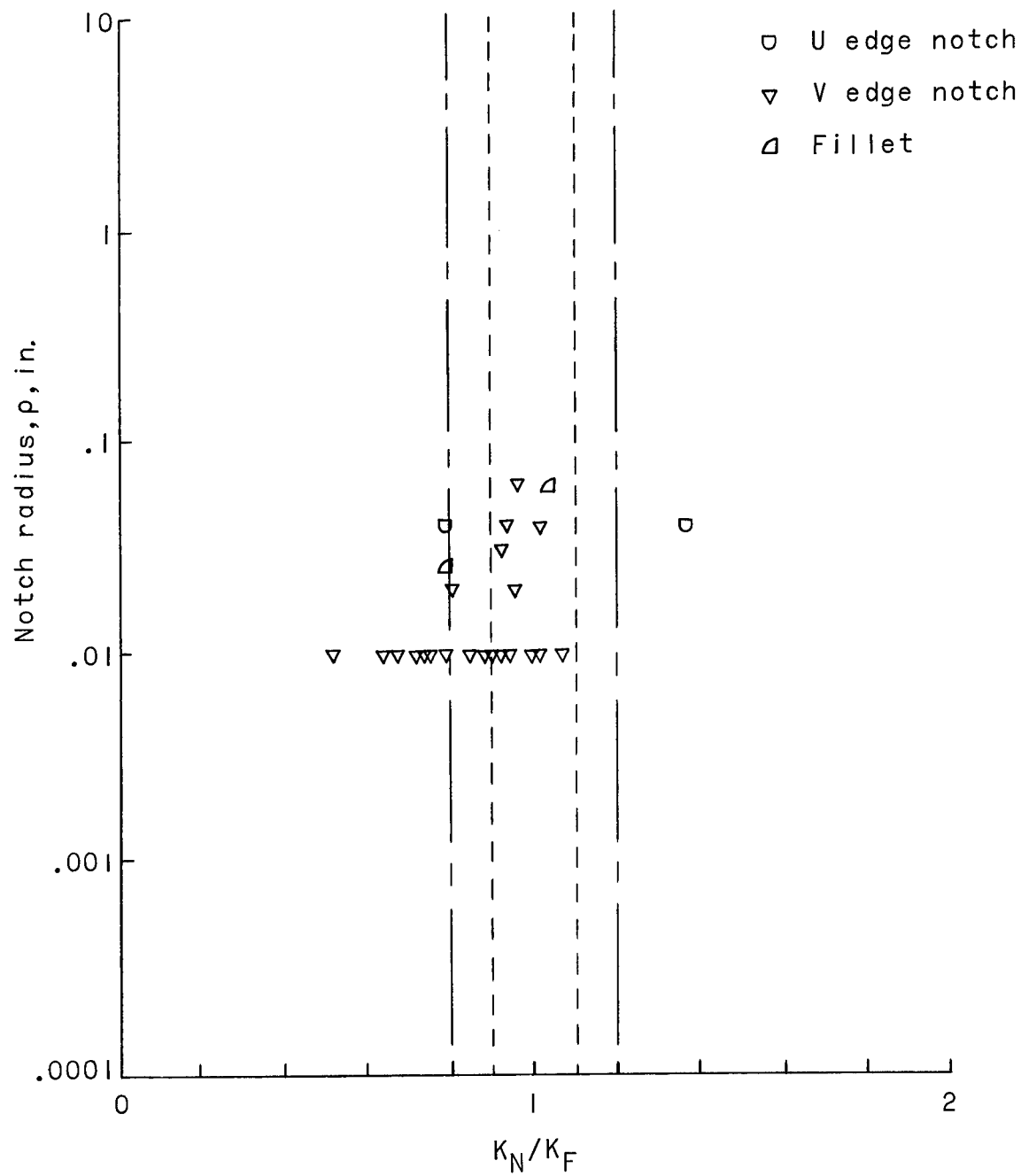
L-1743

(f) Miscellaneous aluminum-alloy specimens, rotating beam.

Figure 10.- Concluded.
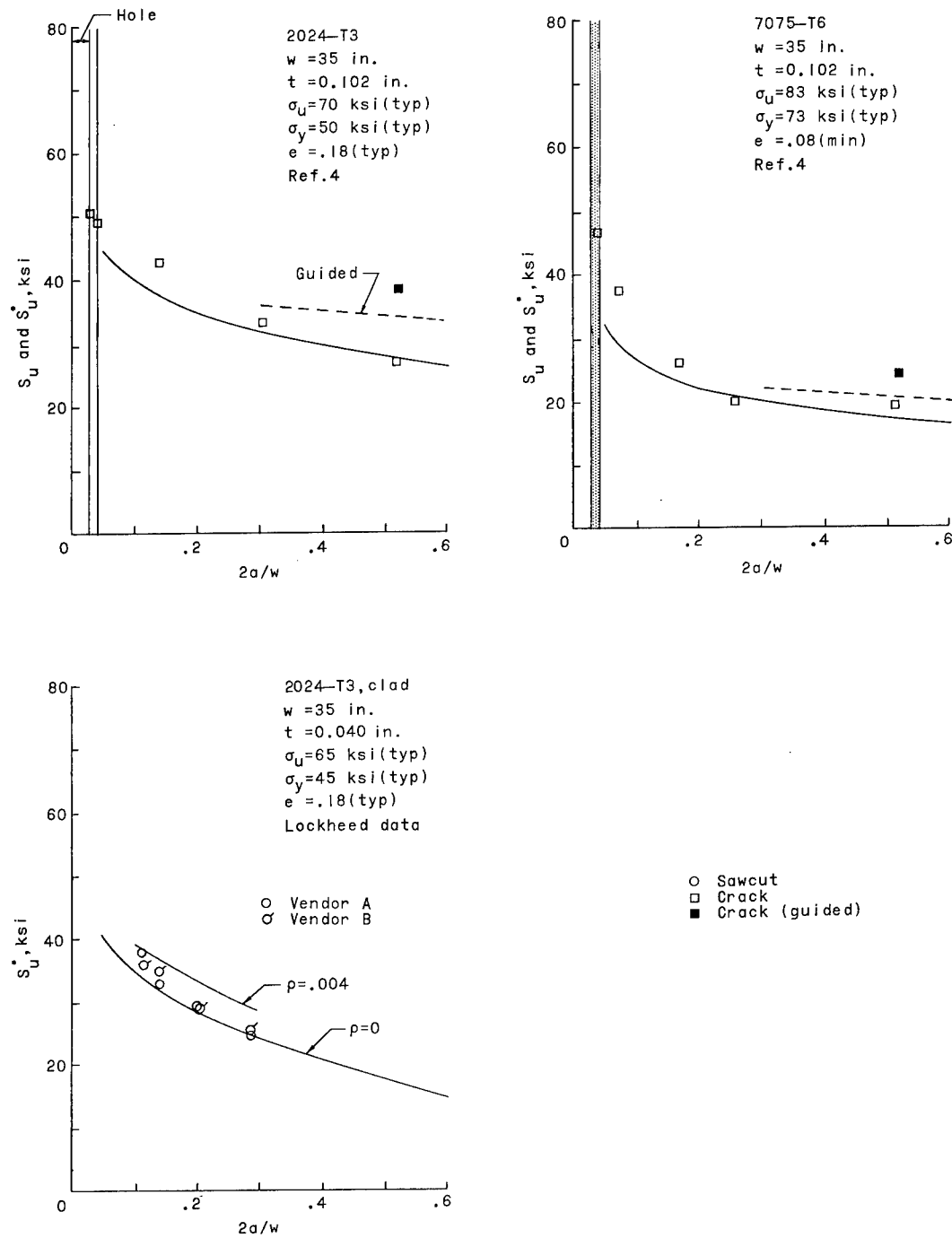
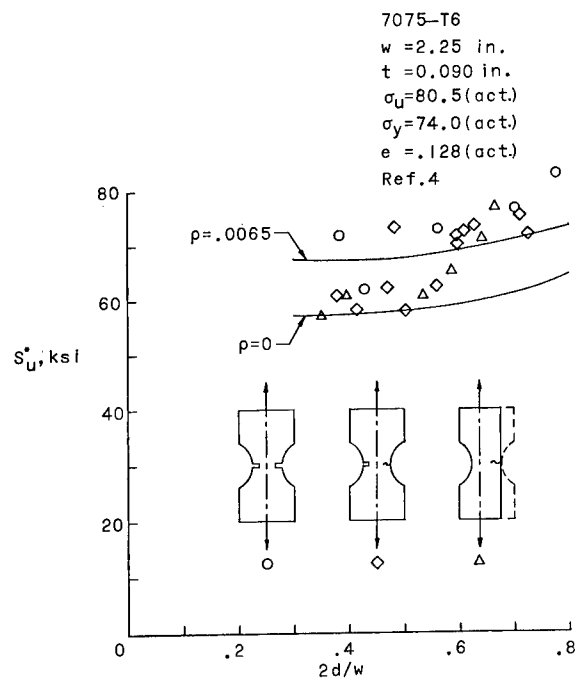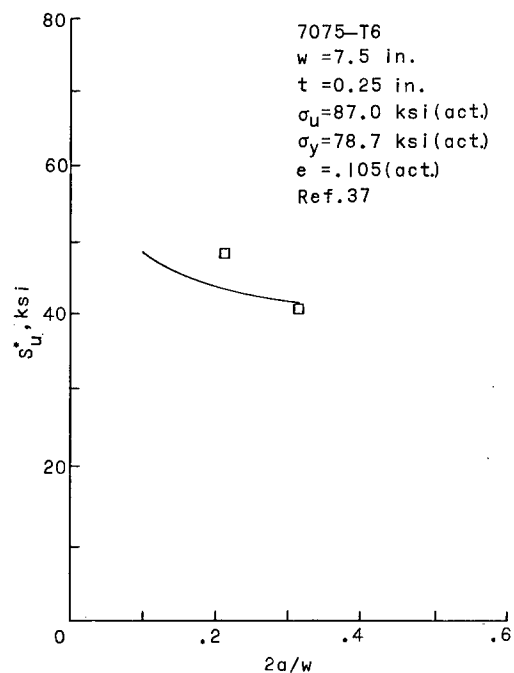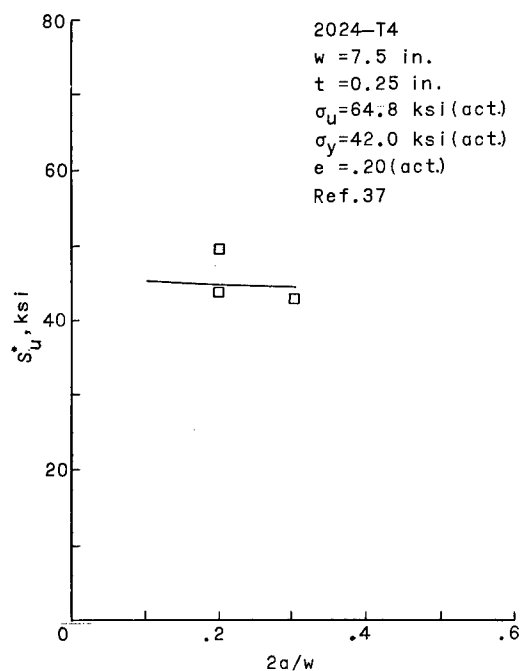(a)

Figure 11.- Strength of sheet material with a crack.

o Sawcut

80 | 2024—T3 clad
w =30 in.
t =0.040 in.
σ_u=65 ksi(typ)
σ_y=45 ksi(typ)
e =.18(typ)
Ref. 34

S_u^*, ksi

40 ρ=.005

ρ=0

20

0 .2 .4 .6
2a/w

80 | 7075—T6 clad
w =30 in.
t =0.040 in.
σ_u=76 ksi(typ)
σ_y=67 ksi(typ)
e =.08(min)
Ref.34

S_u^*, ksi

40 ρ=.005

ρ=0

20

0 .2 .4 .6
2a/w

80 | 2024—T3 clad
w =20 in.
t =0.040,0.091 in.
σ_u=65 ksi(typ)
σ_y=45 ksi(typ)
e =.18(typ)
Lockheed data

S_u^*, ksi

ρ=.004

ρ=0

40

20

0 .2 .4 .6
2a/w

80 | 7075—T6,clad
w =20 in.
t =0.040,0.091 in.
σ_u=76 ksi(typ)
σ_y=67 ksi(typ)
e =.08(min)
Lockheed data

S_u^*, ksi

ρ=.004

ρ=0

40

20

0 .2 .4 .6
2a/w

L-1743

(b)

Figure 11.- Continued.

L-1743

○ Sawcut
□ Crack

2024-T3
w =12 in.
t =0.081 in.
σ_u=70 ksi(typ)
σ_y=50 ksi(typ)
e =.18(typ)
Ref.4

7075-T6
w =12 in.
t =0.075 in.
σ_u=83 ksi(typ)
σ_y=73 ksi(typ)
e =.08(min), .11(typ)
Ref.4

2024-T3,clad
w =9 in.
t =0.040,0.091 in.
σ_u=65 ksi(typ)
σ_y=45 ksi(typ)
e =.18(typ)
Lockheed data

7075-T6,clad
w =9 in.
t =0.040,0.091 in.
σ_u=76 ksi(typ)
σ_y=67 ksi(typ)
e =.08(min)
Lockheed data

(c)

Figure 11.- Continued.

(d)

Figure 11.- Continued.

L-1743

2024—T3
w =2.25 in.
t =0.081,0.090 in.
σ_u=71.9(act.)
σ_y=52.7(act.)
e =.195(act.)
Ref.4

7075—T6
w =2.25 in.
t =0.090 in.
σ_u=80.5(act.)
σ_y=74.0(act.)
e =.128(act.)
Ref.4
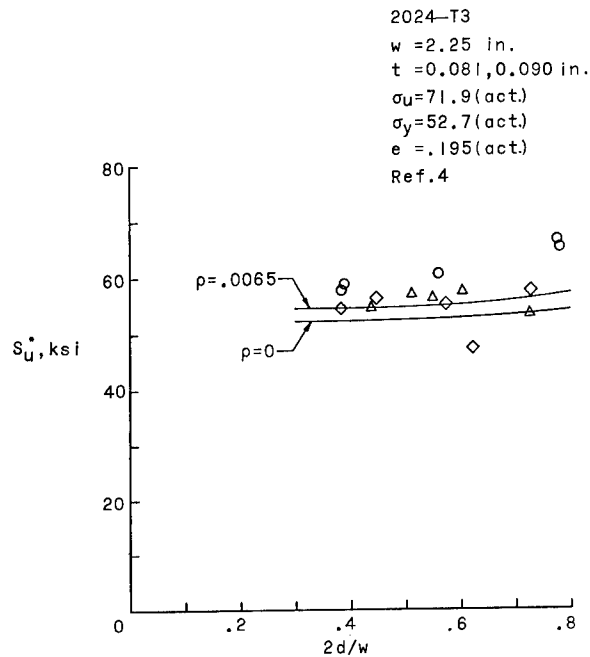
(e)

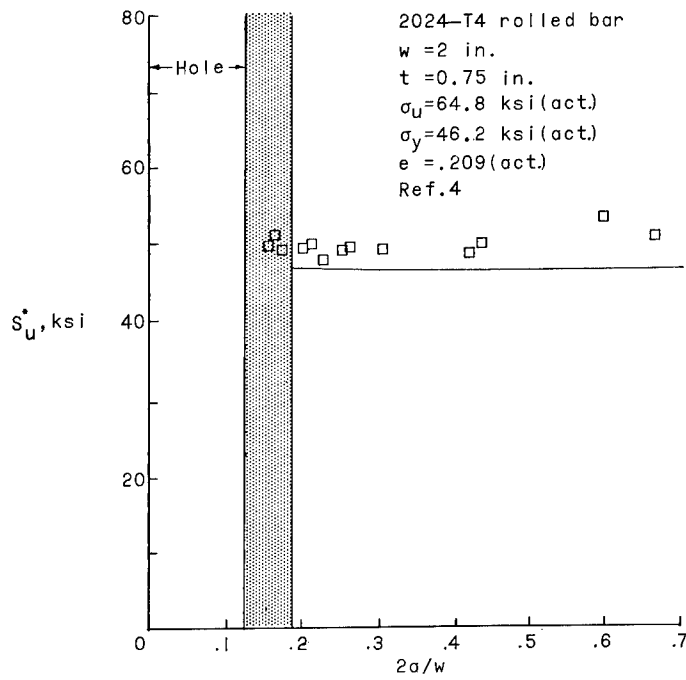Figure 11.- Concluded.
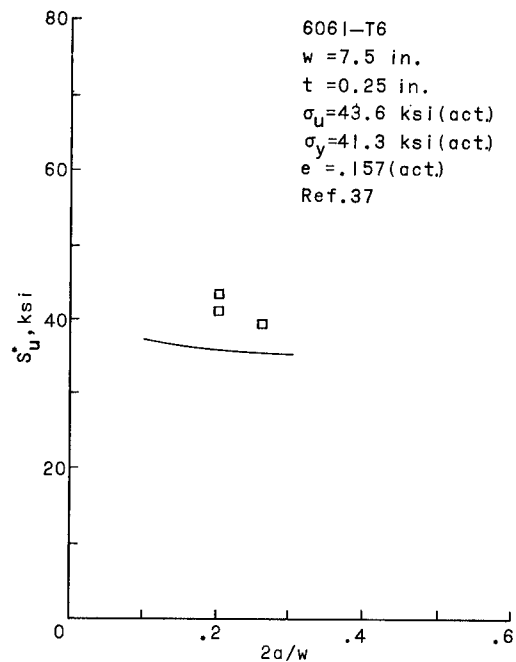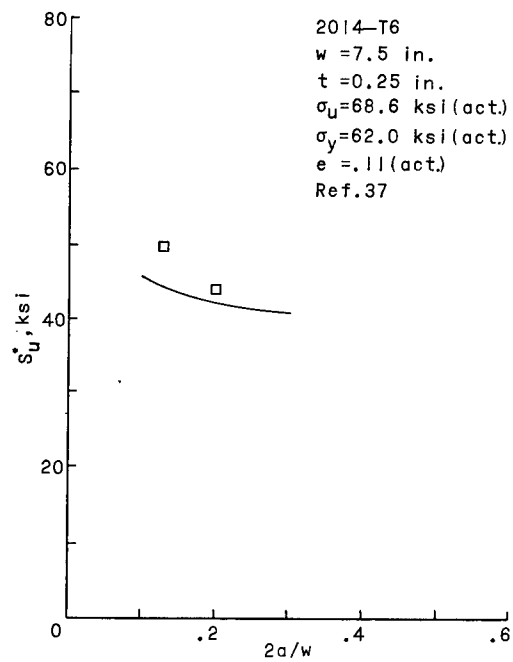
Figure 12.- Strength of plate material with a crack.
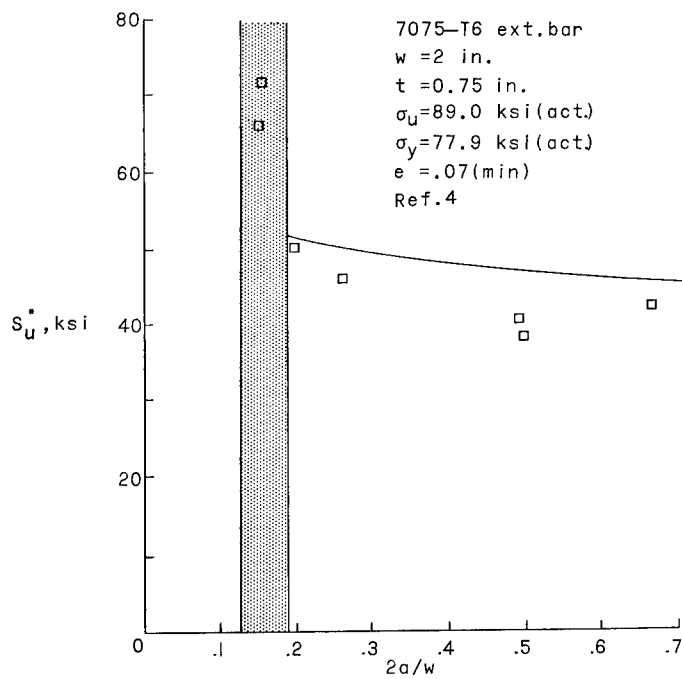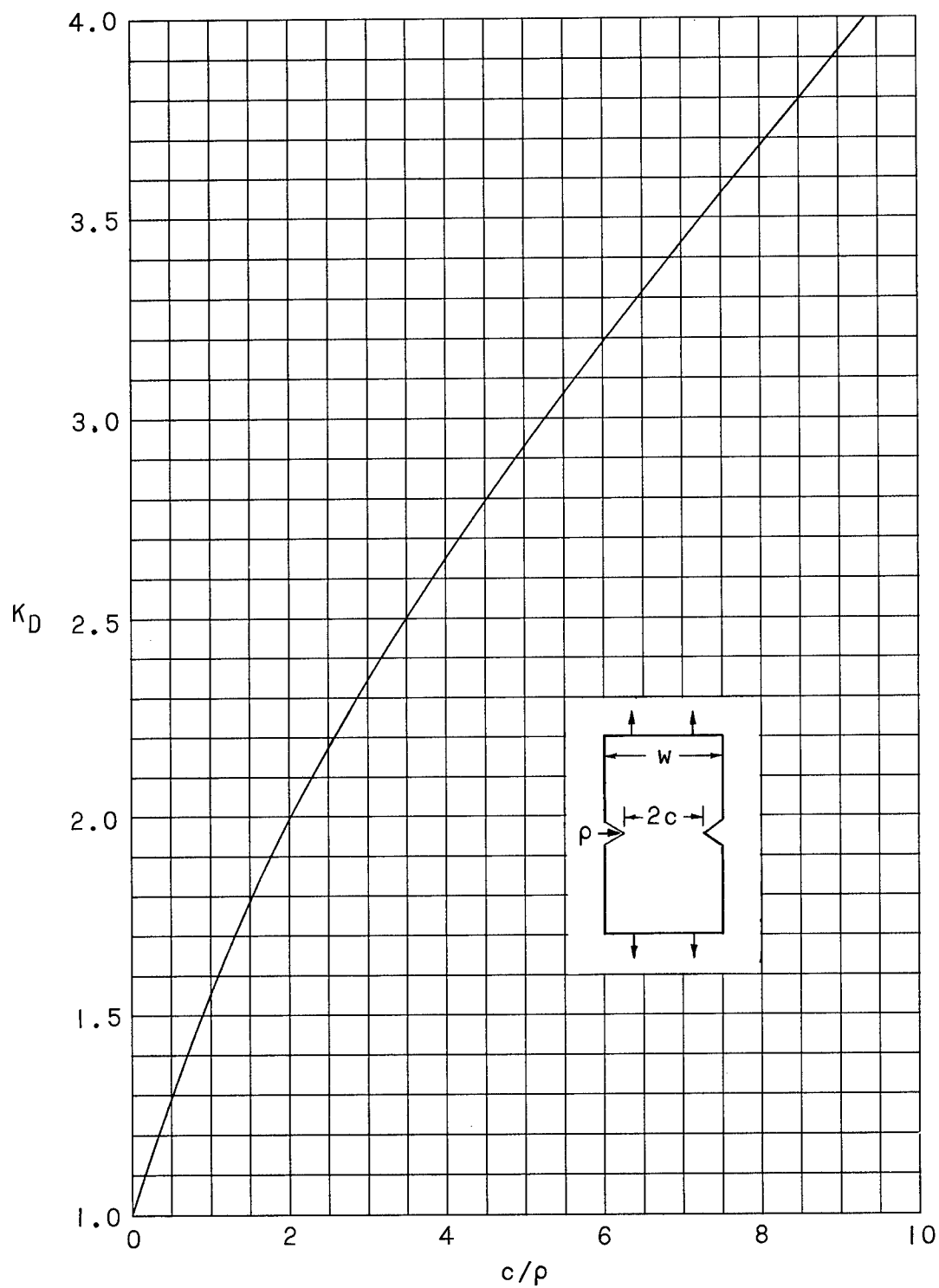
Figure 13.- Strength of bar material with a crack.

L-1743

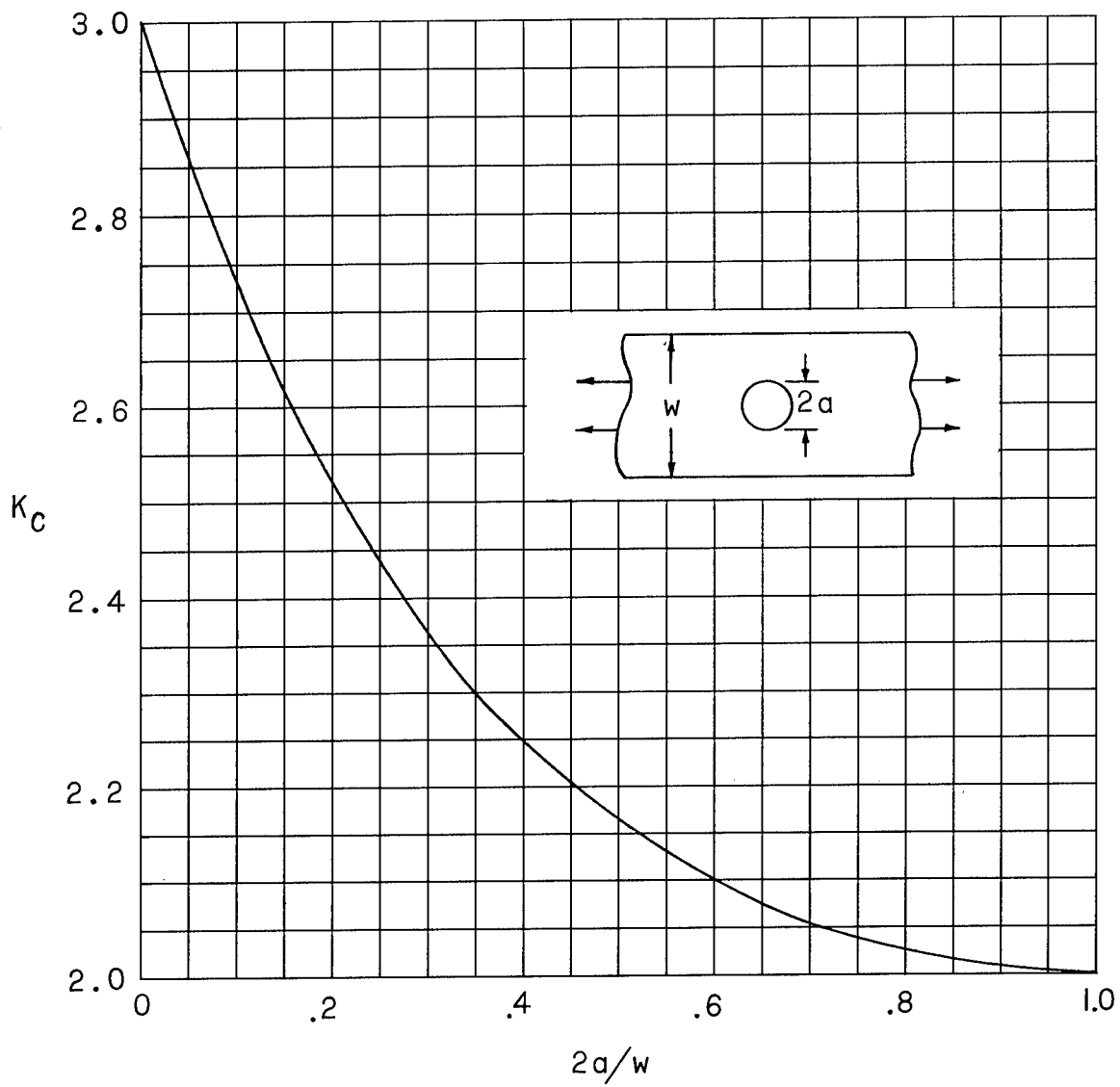Figure 14.- Deep-notch factors for V-notches on sheet in tension.

Figure 15.- Stress-concentration factors for circular holes.

NASA TN D-1259
National Aeronautics and Space Administration.
UNIFIED NOTCH-STRENGTH ANALYSIS FOR
WROUGHT ALUMINUM ALLOYS. Paul Kuhn and
I. E. Figge. May 1962. 76p. OTS price, $2.00.
(NASA TECHNICAL NOTE D-1259)

A simple engineering method is presented for pre-
dicting the strength of notched parts made from
wrought aluminum alloys under static loading or under
repeated loading near the fatigue limit. Assumed to
be known are tensile strength, elongation, and modu-
lus of elasticity; in certain cases, the stress-strain
curve must be known; also needed are "Neuber
constants," which are given in the report. Notch
configurations ranging from mild notches to cracks
are considered. A large number of comparisons
between experimental and predicted results are
presented.

Copies obtainable from NASA, Washington

NASA

I.   Kuhn, Paul
II. Figge, I. E.
III. NASA TN D-1259

(Initial NASA distribution:
25, Materials, engineering;
51, Stresses and loads;
52, Structures.)

NASA TN D-1259
National Aeronautics and Space Administration.
UNIFIED NOTCH-STRENGTH ANALYSIS FOR
WROUGHT ALUMINUM ALLOYS. Paul Kuhn and
I. E. Figge. May 1962. 76p. OTS price, $2.00.
(NASA TECHNICAL NOTE D-1259)

A simple engineering method is presented for pre-
dicting the strength of notched parts made from
wrought aluminum alloys under static loading or under
repeated loading near the fatigue limit. Assumed to
be known are tensile strength, elongation, and modu-
lus of elasticity; in certain cases, the stress-strain
curve must be known; also needed are "Neuber
constants," which are given in the report. Notch
configurations ranging from mild notches to cracks
are considered. A large number of comparisons
between experimental and predicted results are
presented.

Copies obtainable from NASA, Washington

NASA

I.   Kuhn, Paul
II. Figge, I. E.
III. NASA TN D-1259

(Initial NASA distribution:
25, Materials, engineering;
51, Stresses and loads;
52, Structures.)

NASA TN D-1259
National Aeronautics and Space Administration.
UNIFIED NOTCH-STRENGTH ANALYSIS FOR
WROUGHT ALUMINUM ALLOYS. Paul Kuhn and
I. E. Figge. May 1962. 76p. OTS price, $2.00.
(NASA TECHNICAL NOTE D-1259)

A simple engineering method is presented for pre-
dicting the strength of notched parts made from
wrought aluminum alloys under static loading or under
repeated loading near the fatigue limit. Assumed to
be known are tensile strength, elongation, and modu-
lus of elasticity; in certain cases, the stress-strain
curve must be known; also needed are "Neuber
constants," which are given in the report. Notch
configurations ranging from mild notches to cracks
are considered. A large number of comparisons
between experimental and predicted results are
presented.

Copies obtainable from NASA, Washington

NASA

I.   Kuhn, Paul
II. Figge, I. E.
III. NASA TN D-1259

(Initial NASA distribution:
25, Materials, engineering;
51, Stresses and loads;
52, Structures.)

NASA TN D-1259
National Aeronautics and Space Administration.
UNIFIED NOTCH-STRENGTH ANALYSIS FOR
WROUGHT ALUMINUM ALLOYS. Paul Kuhn and
I. E. Figge. May 1962. 76p. OTS price, $2.00.
(NASA TECHNICAL NOTE D-1259)

A simple engineering method is presented for pre-
dicting the strength of notched parts made from
wrought aluminum alloys under static loading or under
repeated loading near the fatigue limit. Assumed to
be known are tensile strength, elongation, and modu-
lus of elasticity; in certain cases, the stress-strain
curve must be known; also needed are "Neuber
constants," which are given in the report. Notch
configurations ranging from mild notches to cracks
are considered. A large number of comparisons
between experimental and predicted results are
presented.

Copies obtainable from NASA, Washington

NASA

I.   Kuhn, Paul
II. Figge, I. E.
III. NASA TN D-1259

(Initial NASA distribution:
25, Materials, engineering;
51, Stresses and loads;
52, Structures.)